Large-Scale Pacific Ocean Sea Level and Circulation Changes vs. the PDO Forcing

Bo Qiu and Shuiming Chen

Dept of Oceanography, University of Hawaii, USA

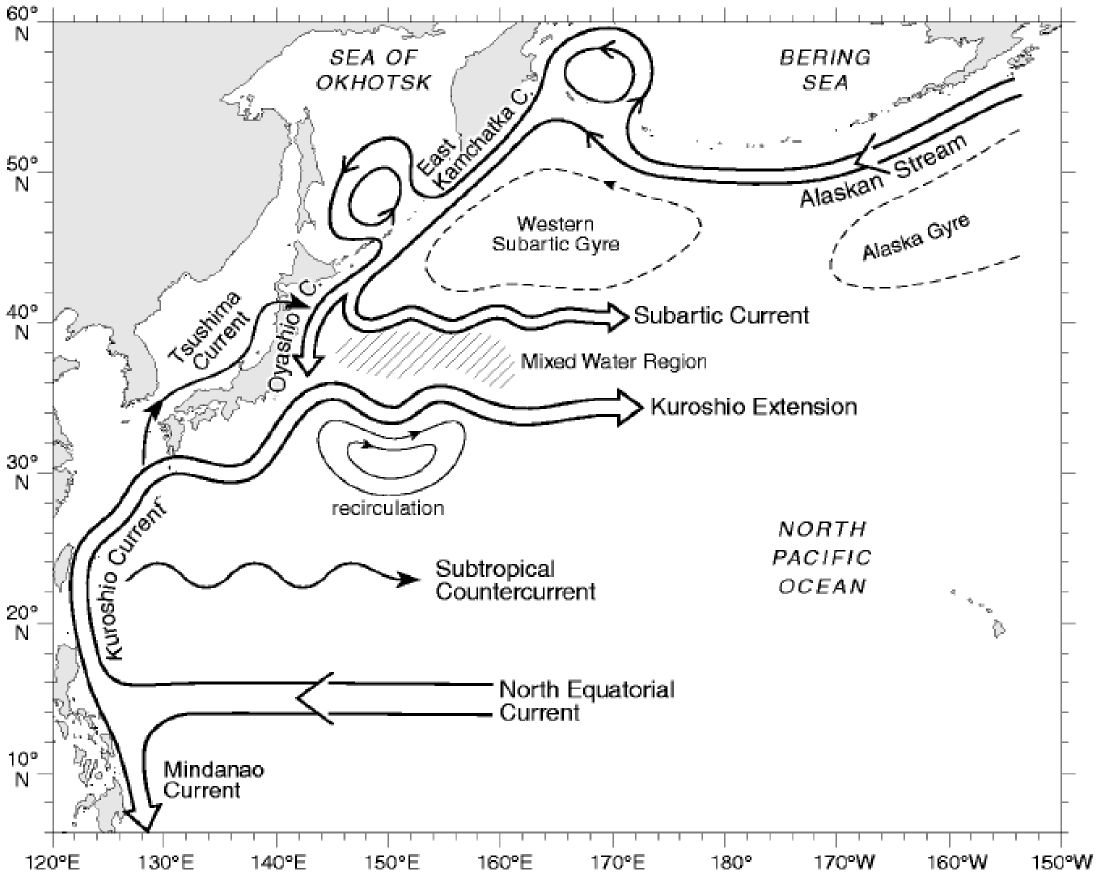

Ocean Surface Topography Science Team Meeting, Boulder, CO, 8-11 October 2013

Outline

- Many recent studies have related the Pacific Ocean sea level and circulation changes to the PDO index
- Sea level and upper ocean circulation changes in different regions are subject to different governing dynamics.
  A deeper understanding of the observed changes requires dynamically-based analyses
- Focus on 3 regions with high variability:
  (a) NEC bifurcation; (b) STCC eddy modulation; and
  (c) Kuroshio Extension dynamical state

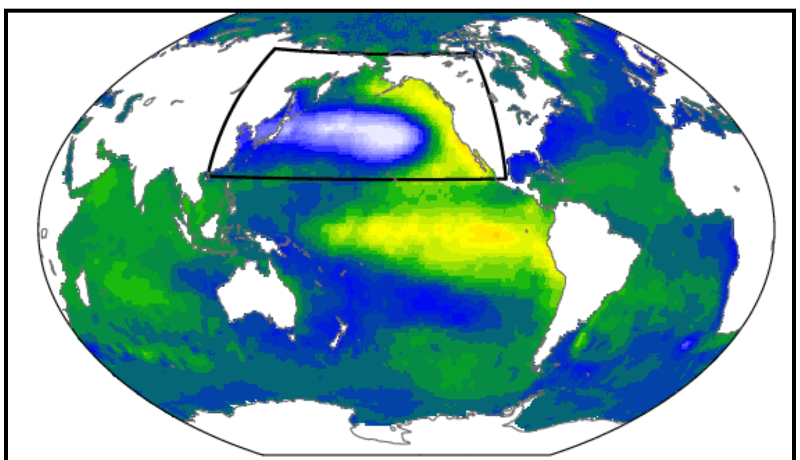

Positive PDO phase (Mantua et al. 1997)

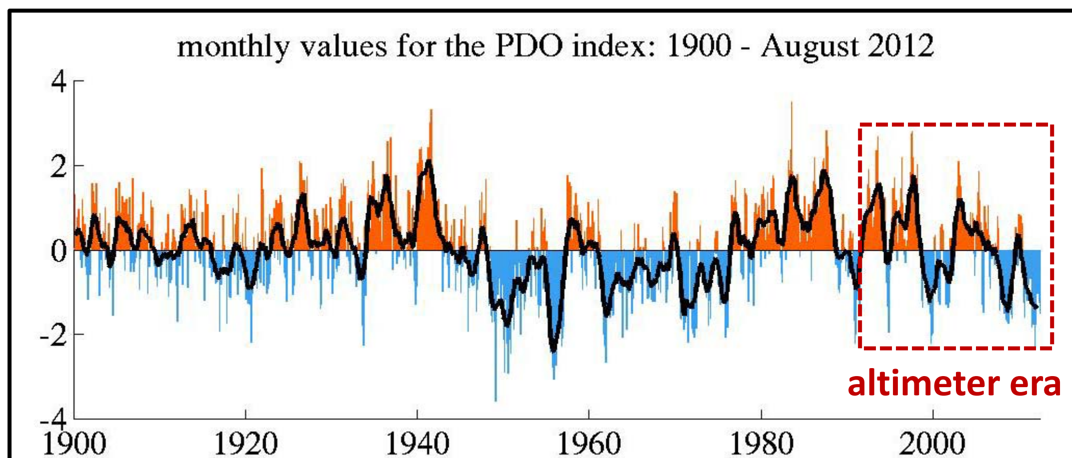

3 dynamically distinct circulation systems in the North Pacific Ocean

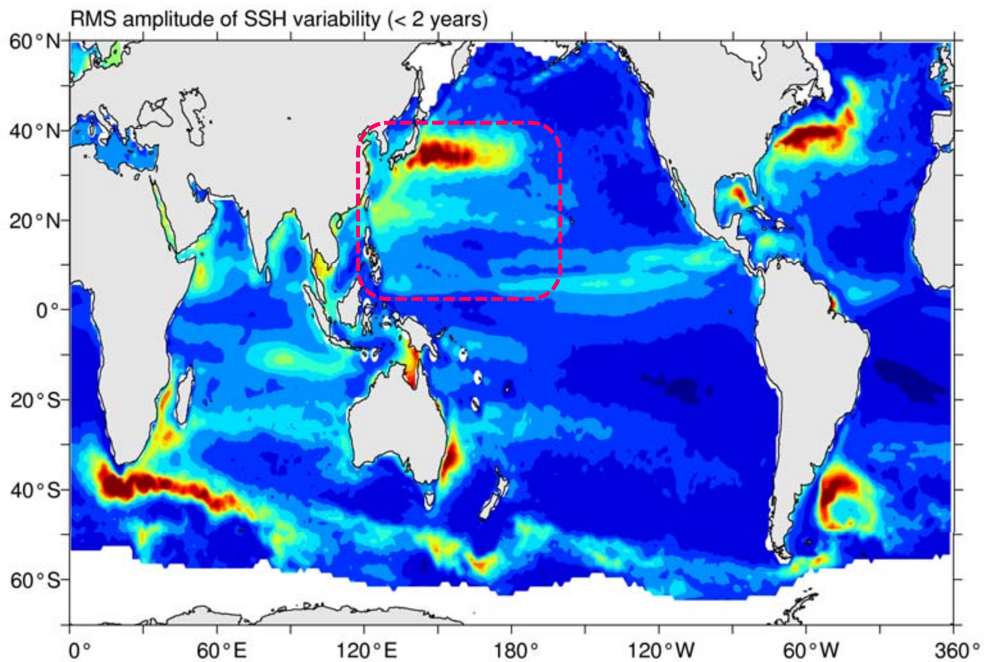

Mesoscale eddy fluctuations

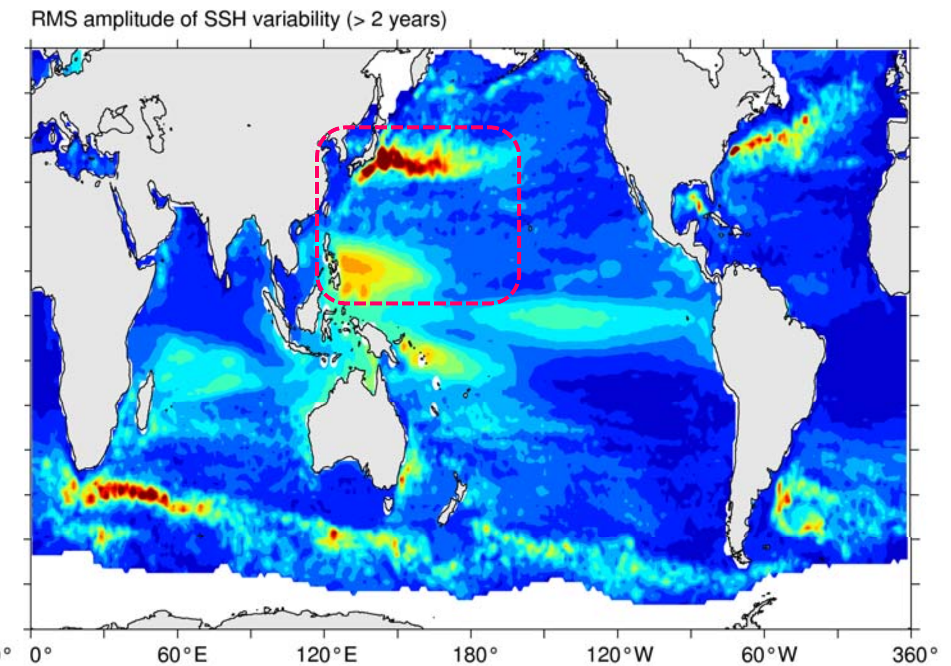

Low-frequency circulation modulations

- **NEC band** (8°-18°N) :
  low EKE level + high decadal circulation changes
- **Subtropical Countercurrent band** (18°-30°N):
  high EKE level + relatively low decadal circulation changes
- **Kuroshio Extension band** (30°-40°N):
  high EKE level + decadal circulation changes

Identifying time-varying NEC bifurcation along the Philippine coast

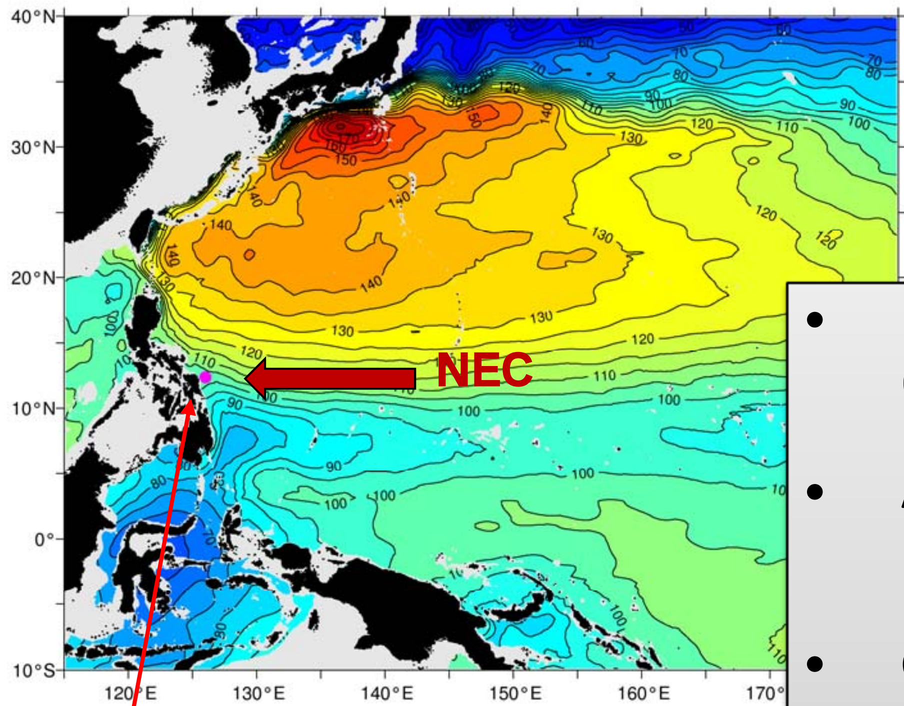

NEC bifurcation latitude = boundary of tropical and subtropical gyres

- Utilize the weekly AVISO SSH anomaly data (1/3°-resolution, 10/1992-present)
- Add the mean SSH field of Rio et al. (2009): mean NEC bifurcation at ~12°N
- Calculate the meridional geostrophic velocity as a function of y along the Philippine coast:

$$v_g(y,t) = \frac{g}{f}\left[h_e(y,t) - h_w(y,t)\right],$$

where h_e is SSH in 1°-band east of the coast and h_w in 1°-band further to the east

- The NEC bifurcation latitude $Y_b(t)$ is defined at where v_g=0 in each month

Time-varying NEC bifurcation latitude inferred from AVISO SSH data

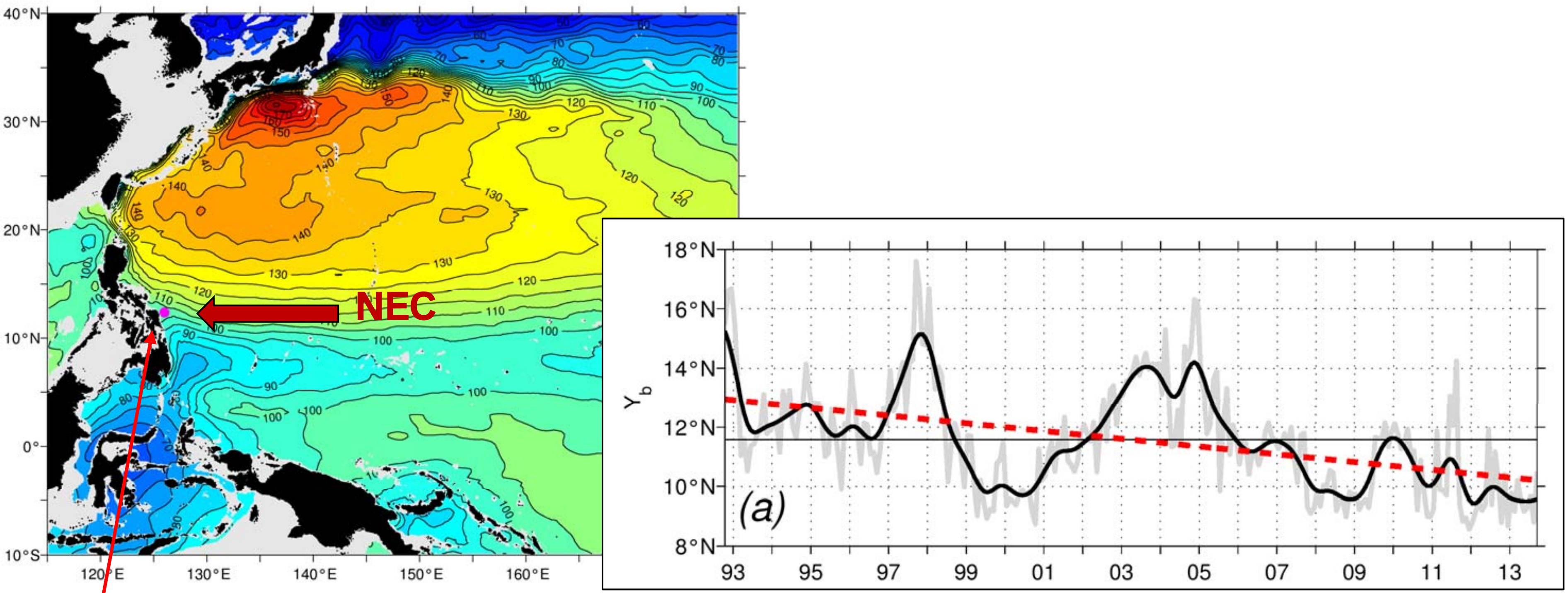

NEC bifurcation latitude
= boundary of tropical and subtropical gyres

- **Presence of intense intra-seasonal signals, representing fluctuations of Mindanao Dome**
- **Large migration of > 6° on interannual timescales**
- **Long-term southward shift with a trend −1.1°/decade**
- **Trend related to the regional enhanced sea level rise and expansion of ST gyre in western Pacific**

Time-varying NEC bifurcation latitude inferred from AVISO SSH data

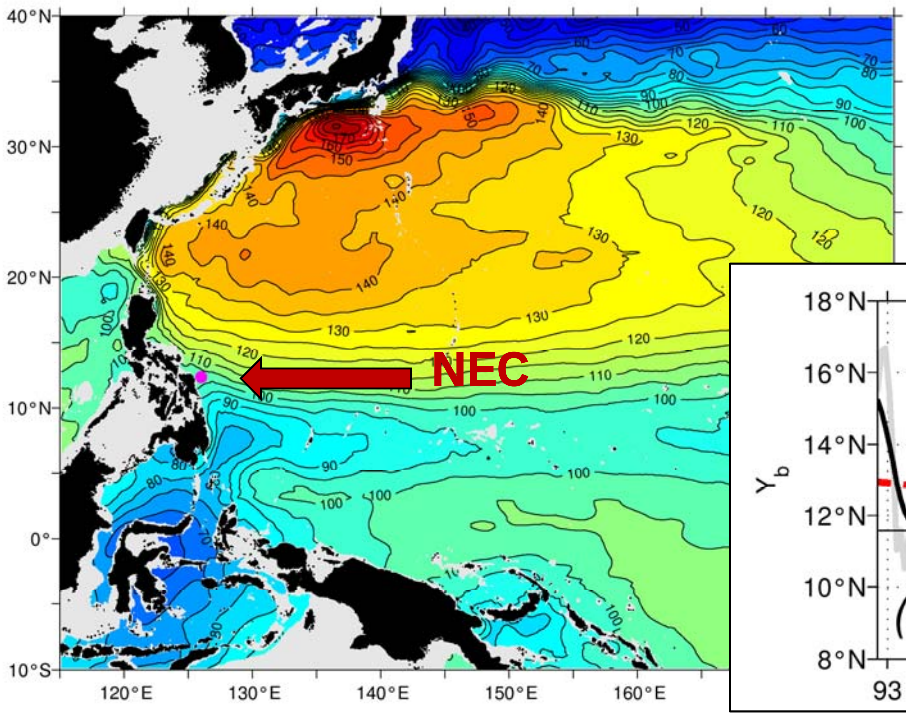

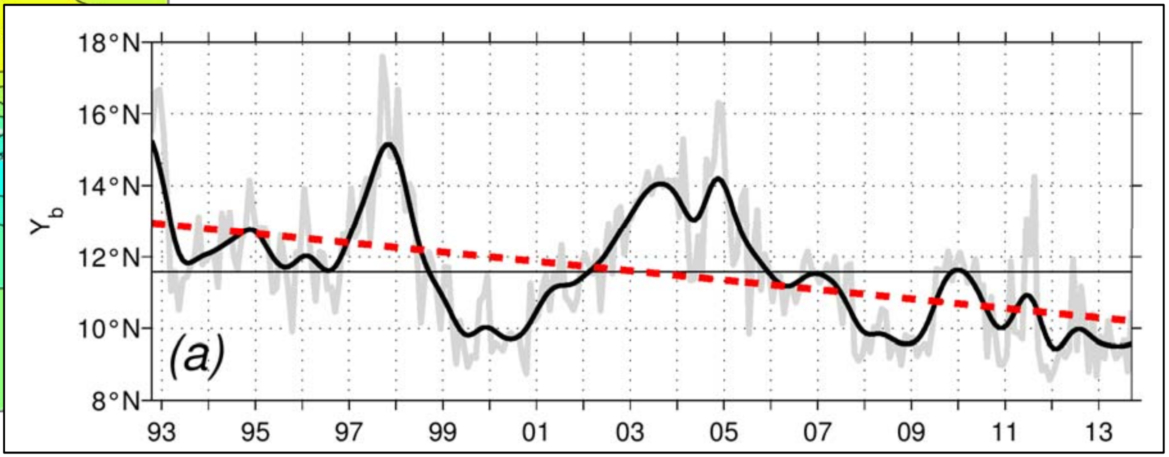

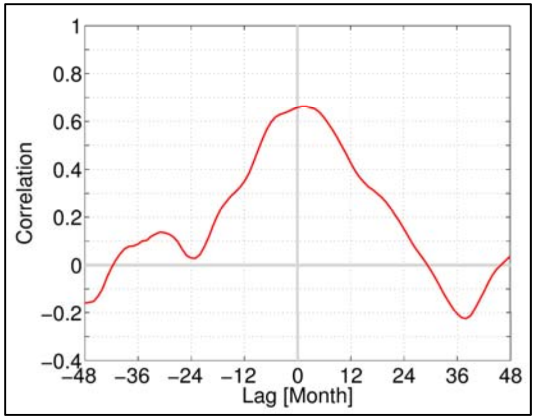

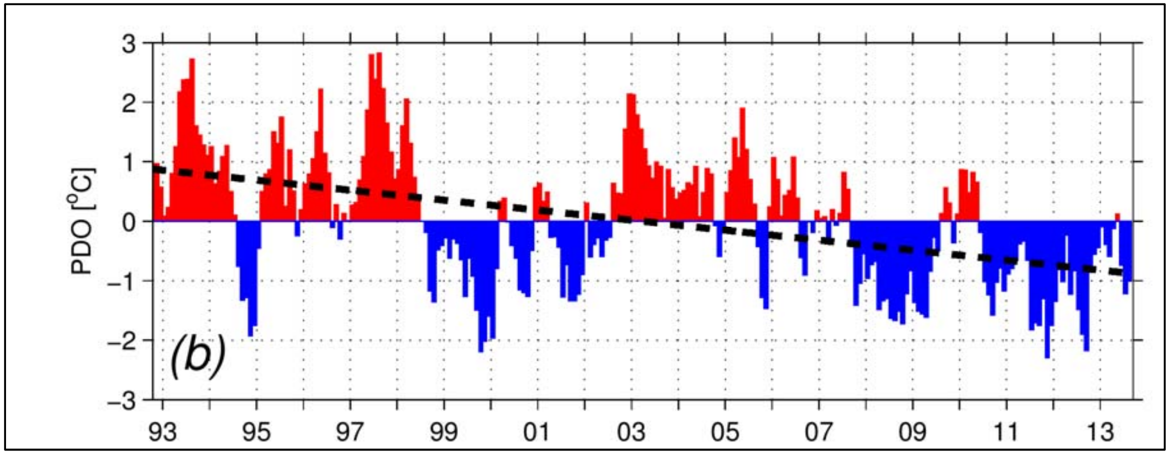

PDO index leads $Y_b(t)$ by ~ 3 months with r = 0.67

Linear correlation between $Y_b(t)$ and local SSH time series

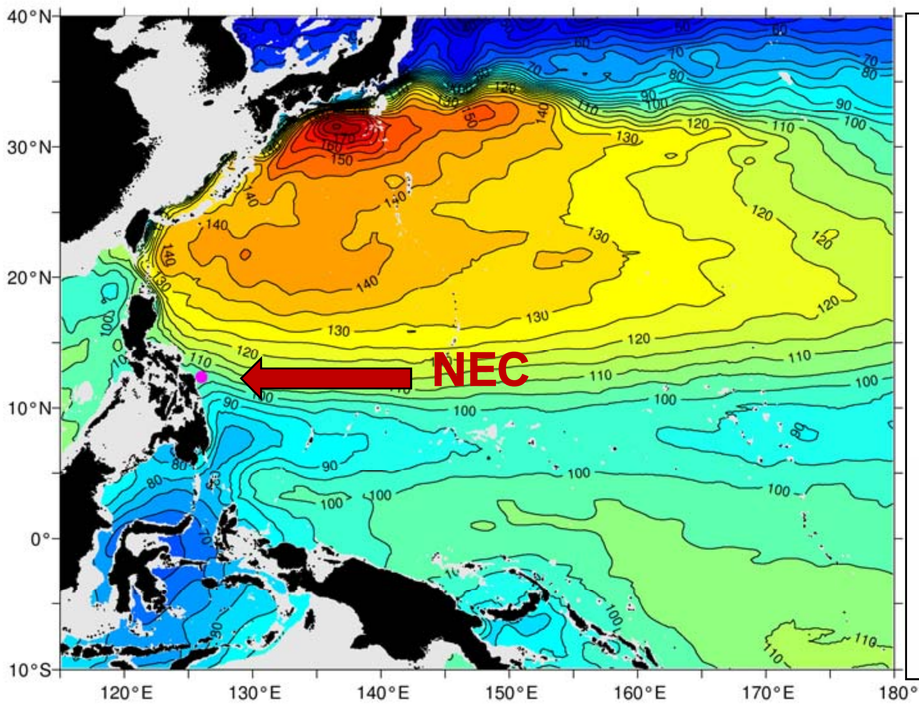

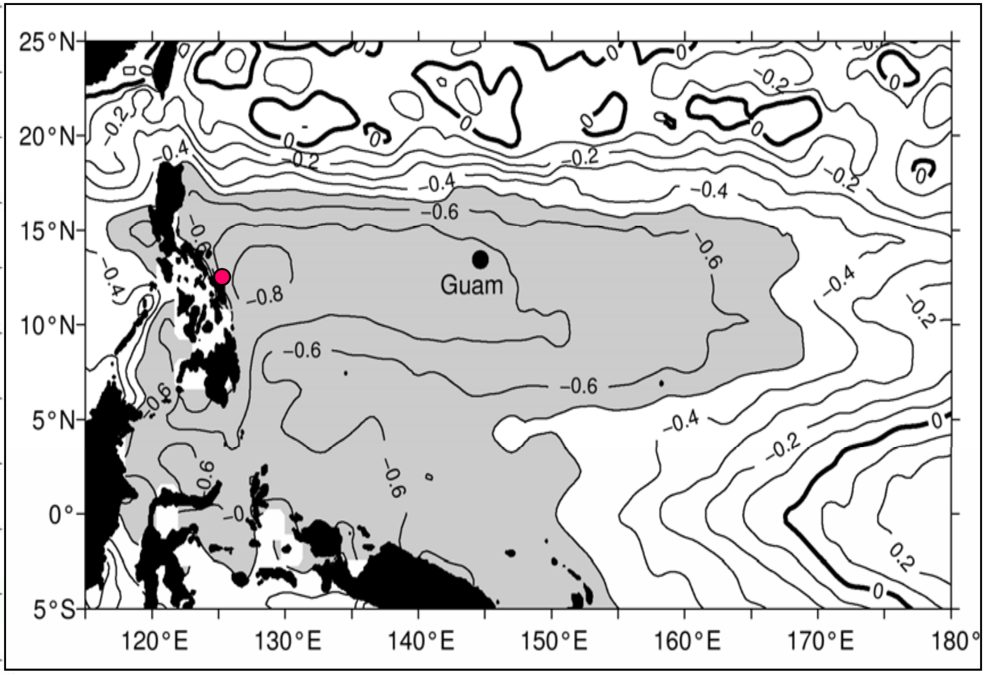

- **NEC bifurcation change is caused by SSH change off the Philippine coast: + SSHA → ST gyre expansion → southward Y_b**

- **Low-frequency SSH variability is dominantly wind-forced:**

$$\frac{\partial h'}{\partial t} - c_R \frac{\partial h'}{\partial x} = -\frac{g' \,\mathrm{curl}\, \boldsymbol{\tau}}{\rho_o g f} - \epsilon h',$$

- **NEC bifurcation change can be quantified by the PDO-wind-forced SSH changes**

x-t plot of observed vs. modeled SSH anomalies along 12°-14°N

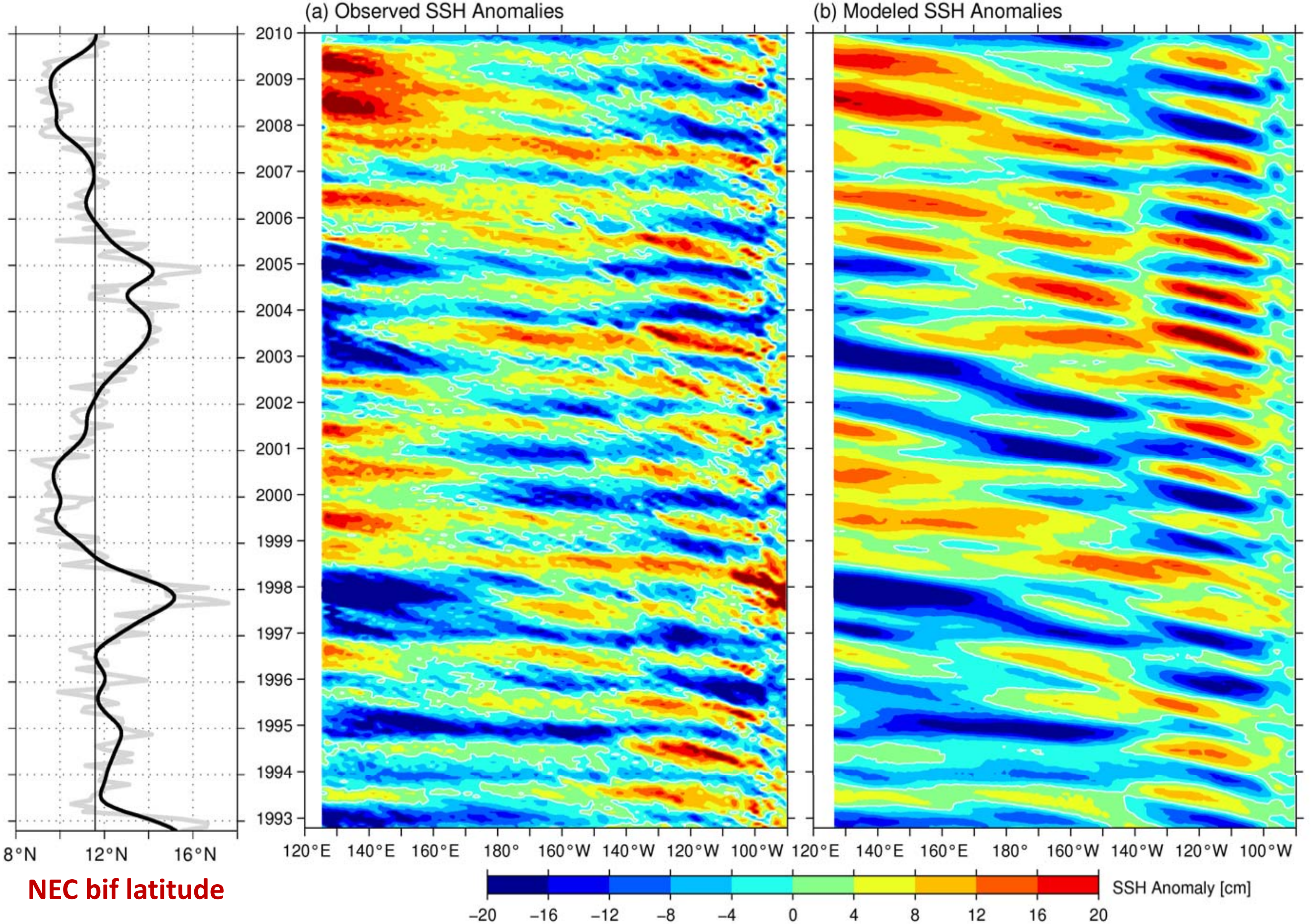

Most of the decadal SSH variability occurs in the western Pacific basin

Wind stress vector and curl (in color) regressed to the PDO index

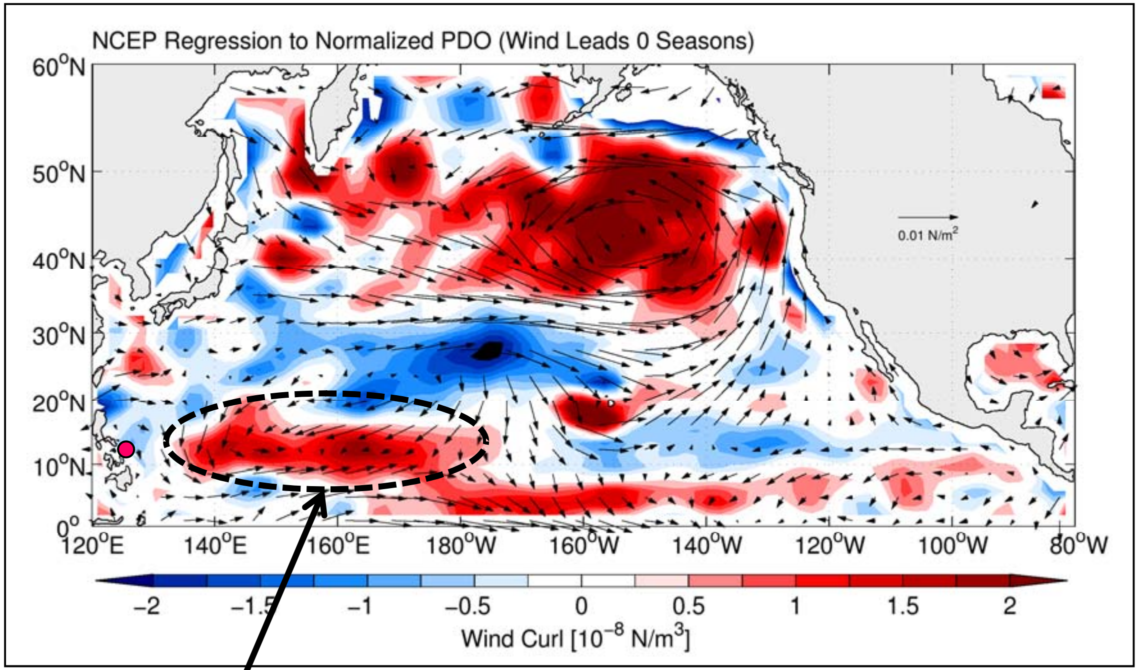

- PDO-induced wind forcing has a **tropical imprint** !
- Its center of action is located in the western basin east of NEC bifurcation → fast and intense Y_b response
- Positive PDO ↔ Ekman flux divergence → negative SSHAs → intensified tropical gyre/northward Y_b shift

Qiu and Chen (2012, JPO)

Wind stress vector and curl (in color) regressed to the PDO index

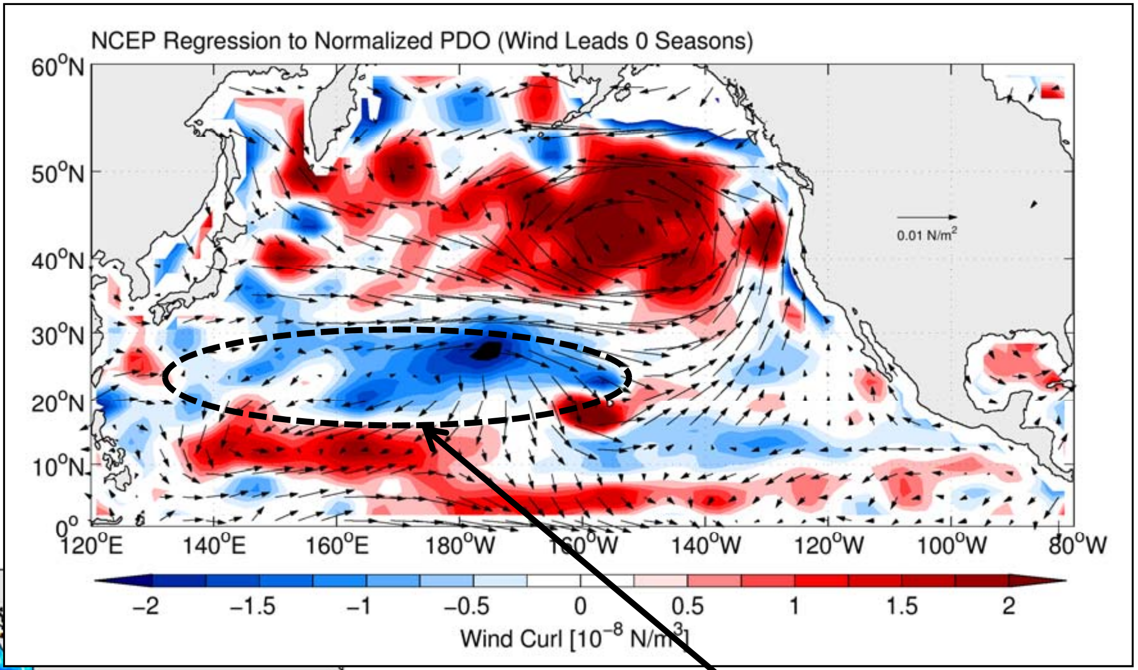

PDO-induced wind forcing has an overlying negative curl along the STCC band

rms SSH variability in N Pacific

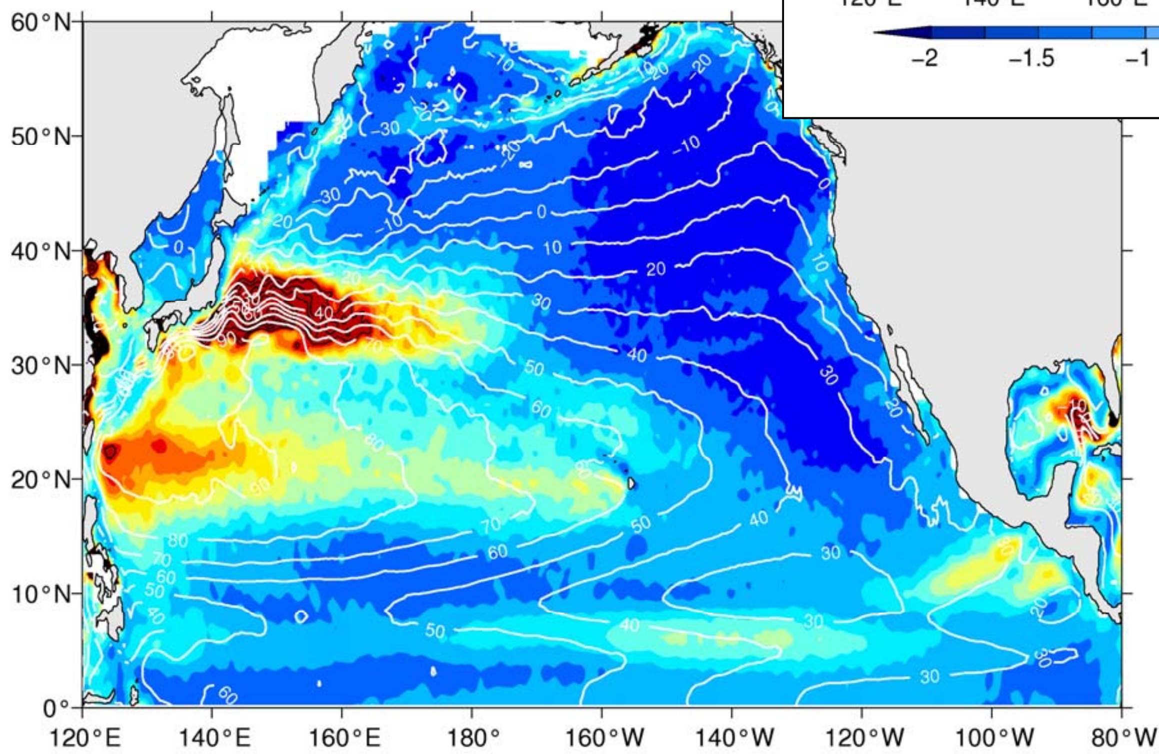

Enhanced eddy variability along STCC due to baroclinic instability

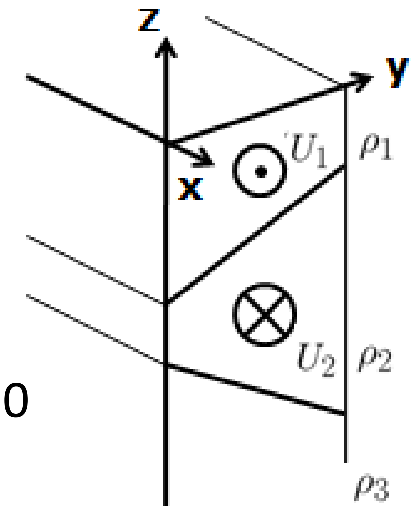

$\Pi_{1y}\Pi_{2y}<0$

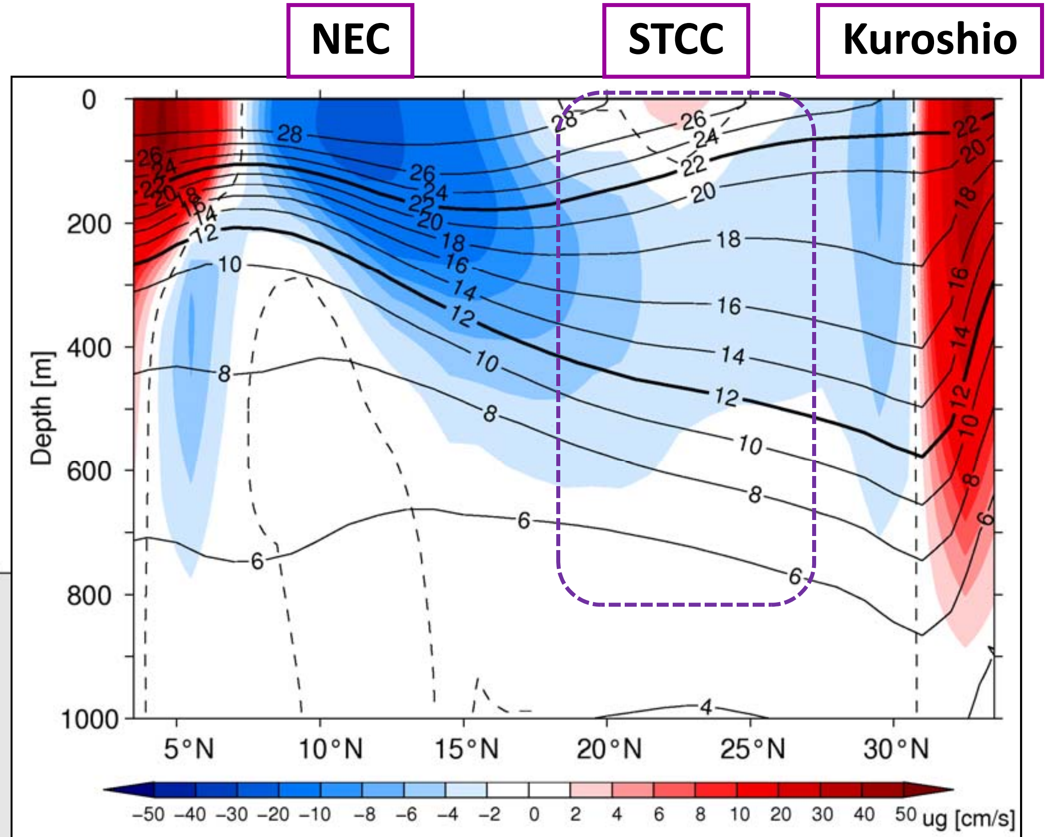

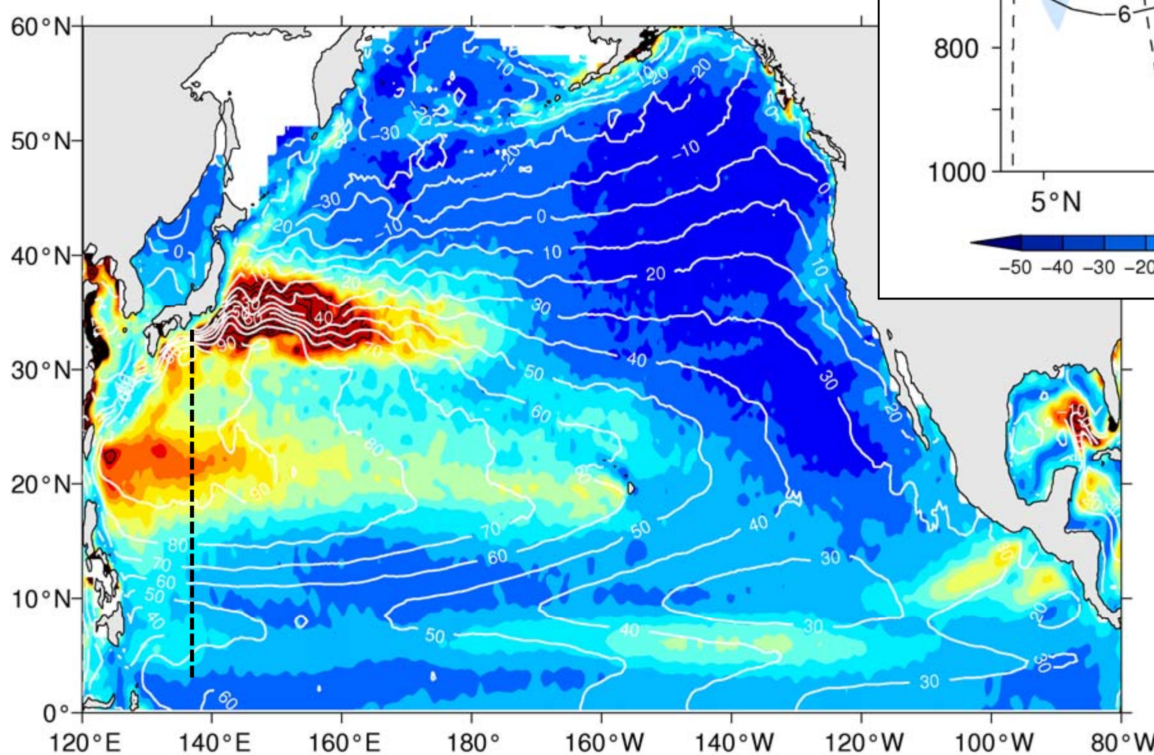

JMA temperature and Ug section along 137°E (1993-2008 mean)

EKE time series in the STCC band: 18°-25°N, 135°-170°E

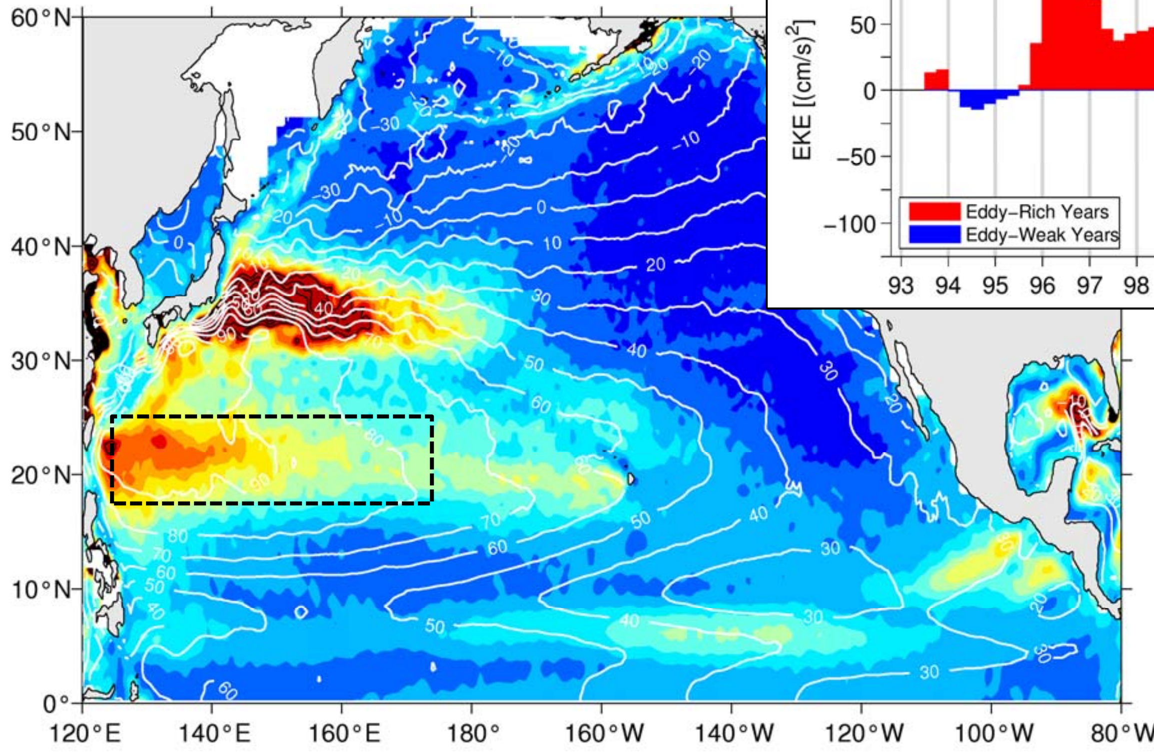

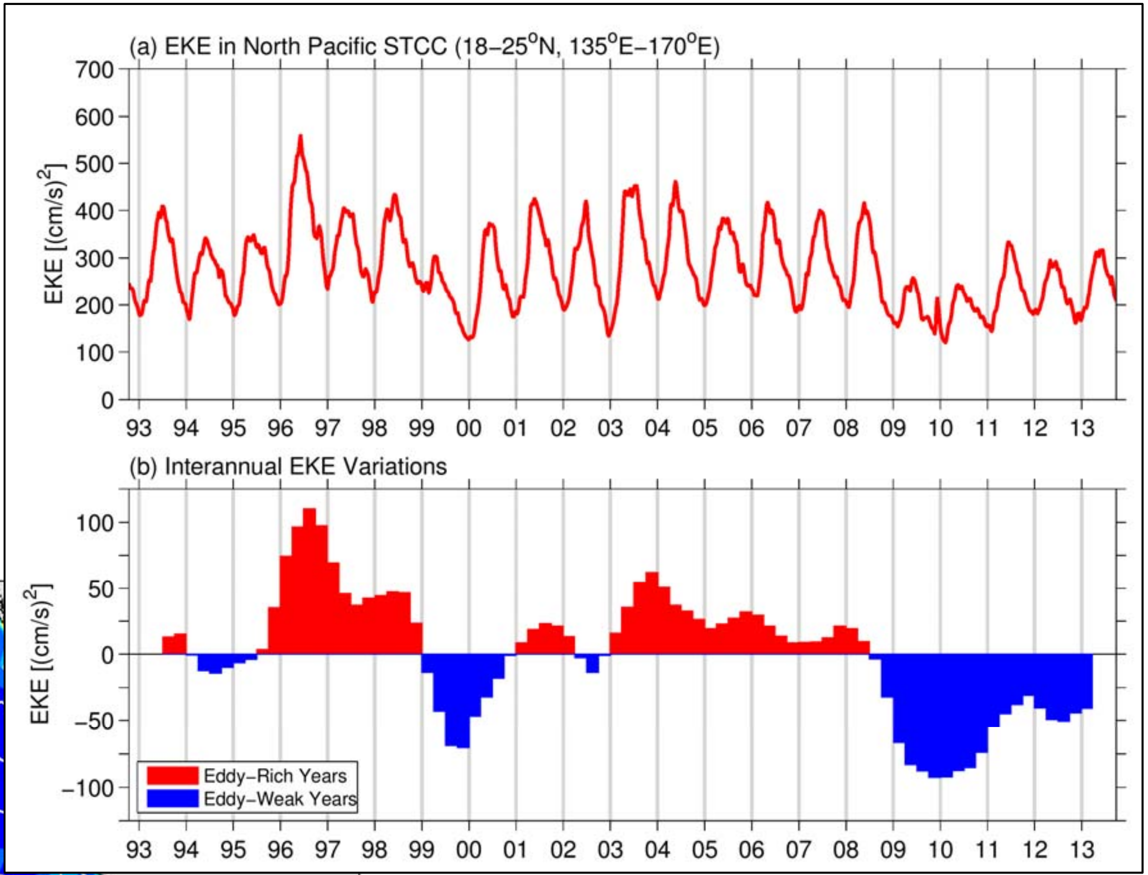

In addition to a well-defined annual cycle, decadal modulations are prominent

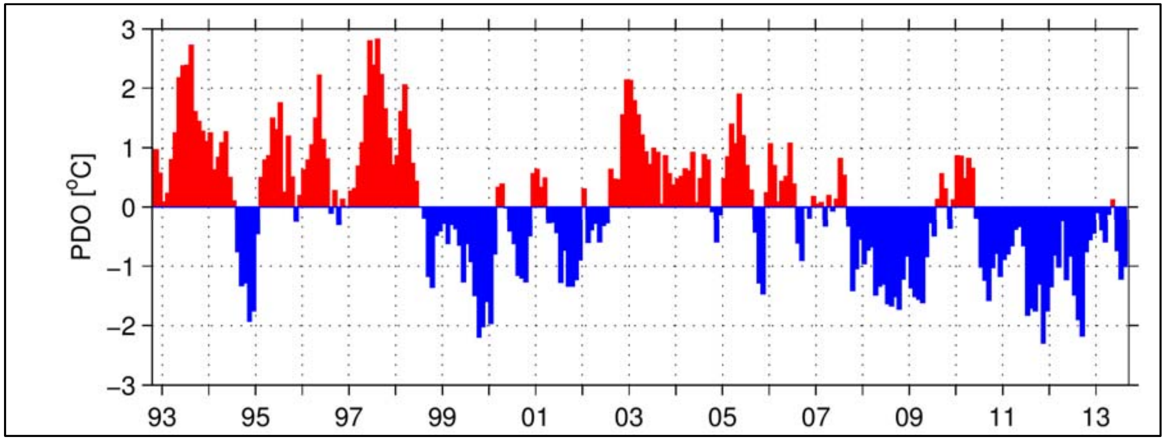

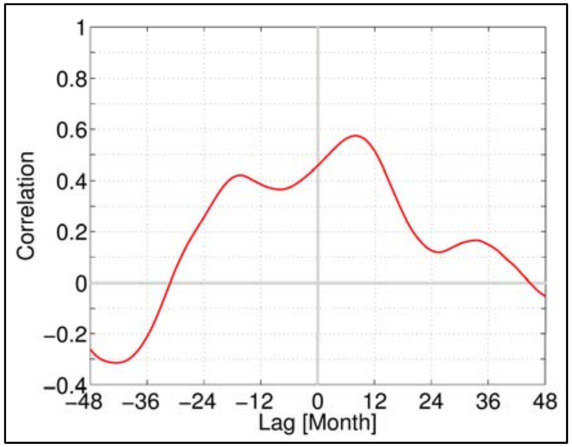

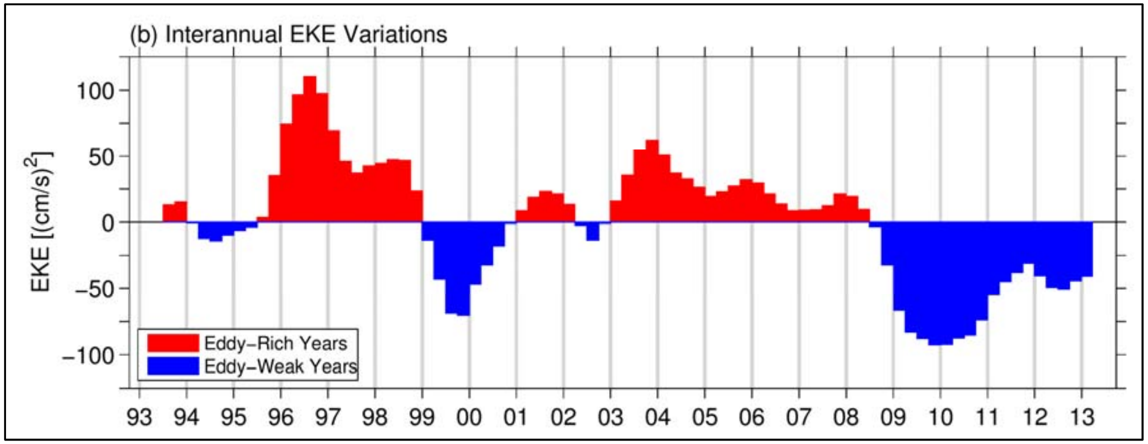

Decadal EKE signals lag the PDO index by ~9 months

Differences in EKE and upper 150m ocean $\partial U_g/\partial z$: 2003-06 minus 2009-11

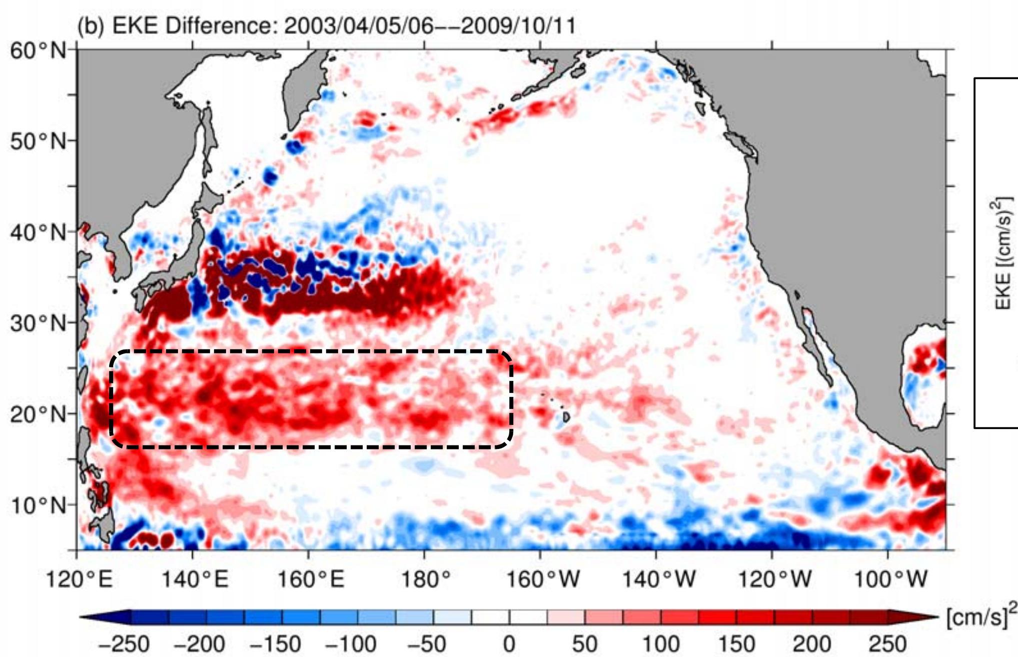

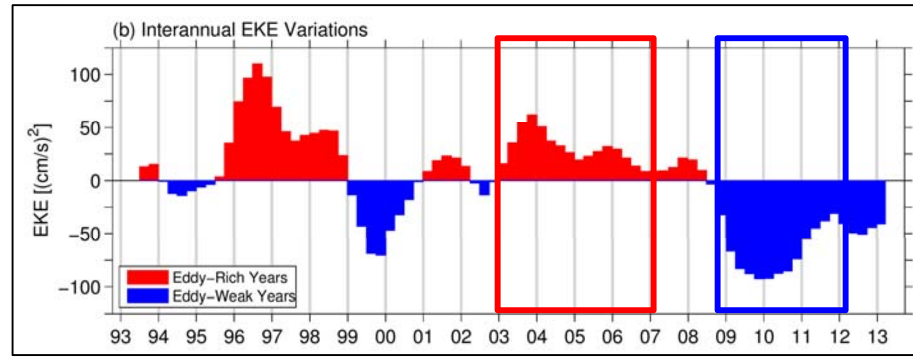

Enhanced EKE signals are due to greater upper ocean vertical shear, hence the baroclinic instability of the sheared STCC/NEC system

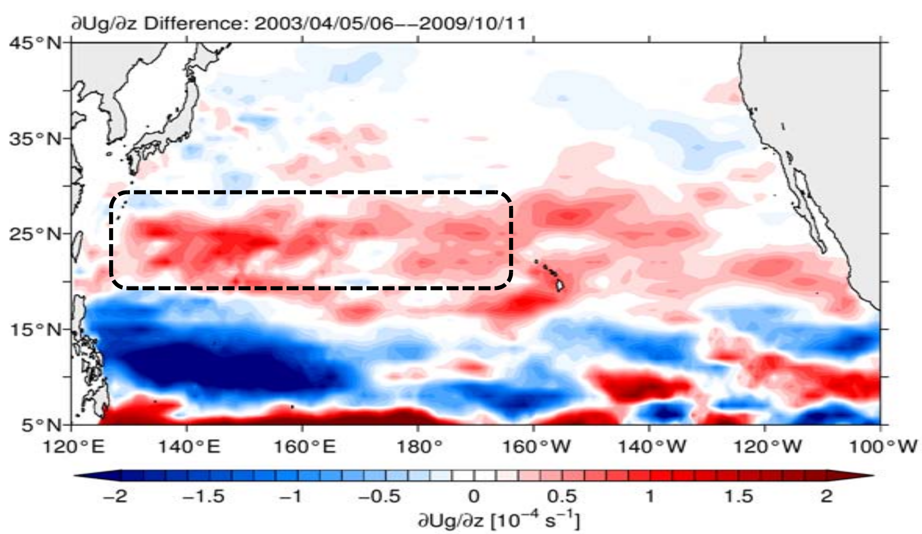

$$\text{EKE} \propto \frac{\partial U_g}{\partial z}$$

Based on the Argo dataset compiled by Hosoda et al. (2008)

Wind stress vector and curl (in color) regressed to the PDO index

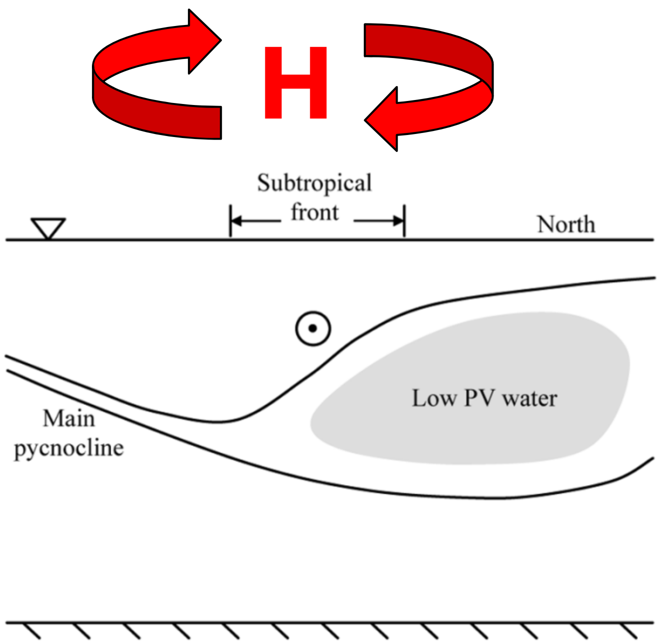

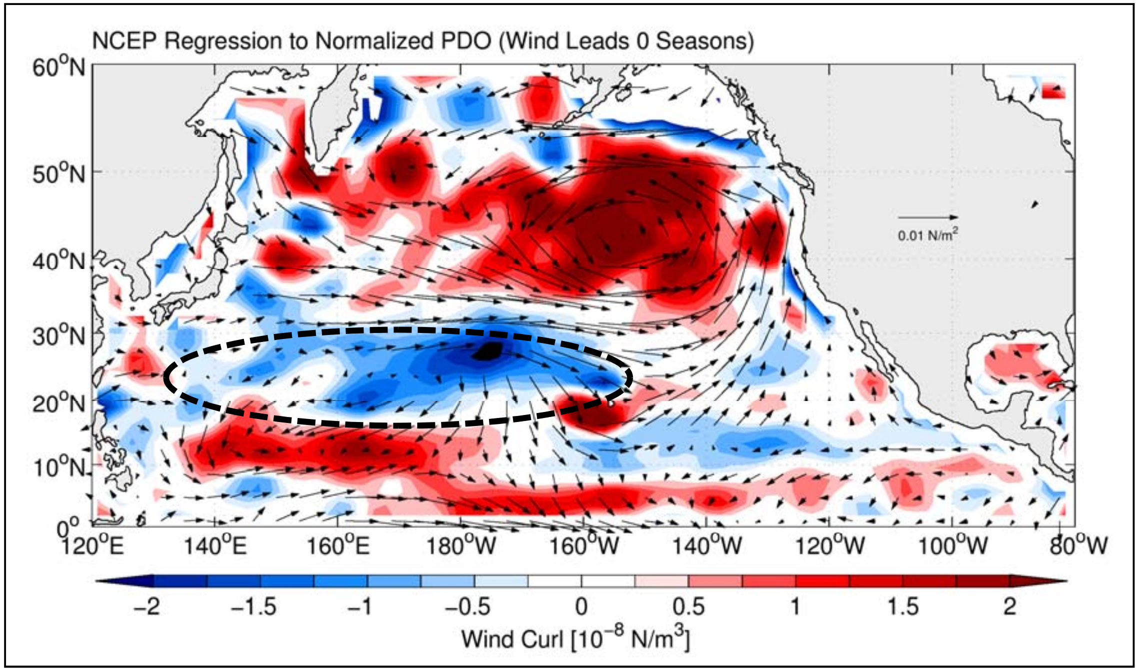

$$\frac{\partial}{\partial t}\left(\langle\frac{\partial U_g}{\partial z}\rangle\right) = \frac{\alpha g}{f}\frac{\partial}{\partial y}\left(\langle \mathbf{u}_{Ek}\rangle \cdot \nabla \langle T\rangle\right) - \frac{\alpha g}{f\rho_0 c_p H_0}\frac{\partial Q_{net}}{\partial y}$$

The negative curl results in cold (warm) advection from north (south), enhancing STCC's baroclinic shear.

Stronger westerlies increases heat loss toward the north, also increasing STCC's baroclinic shear.

9-months are the time required for U_g adjustment and growth of baroclinic instability

Qiu and Chen (2013, JPO)

Wind stress vector and curl (in color) regressed to the PDO index

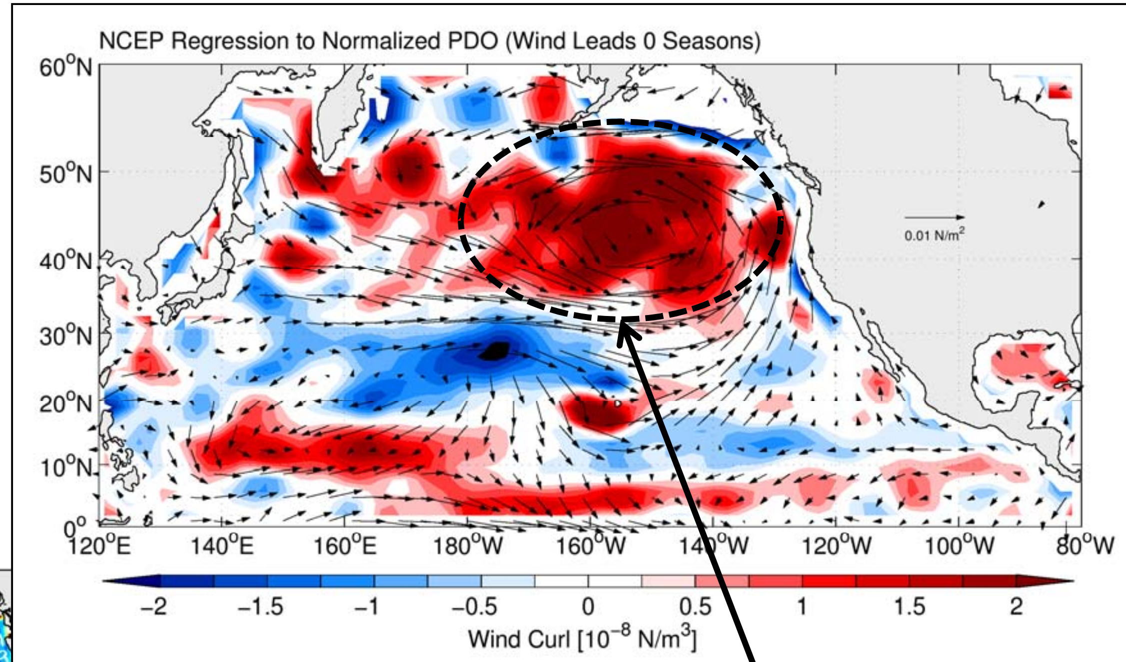

PDO-induced wind forcing has a center of action to the east of the Kuroshio Extension band

rms SSH variability in N Pacific

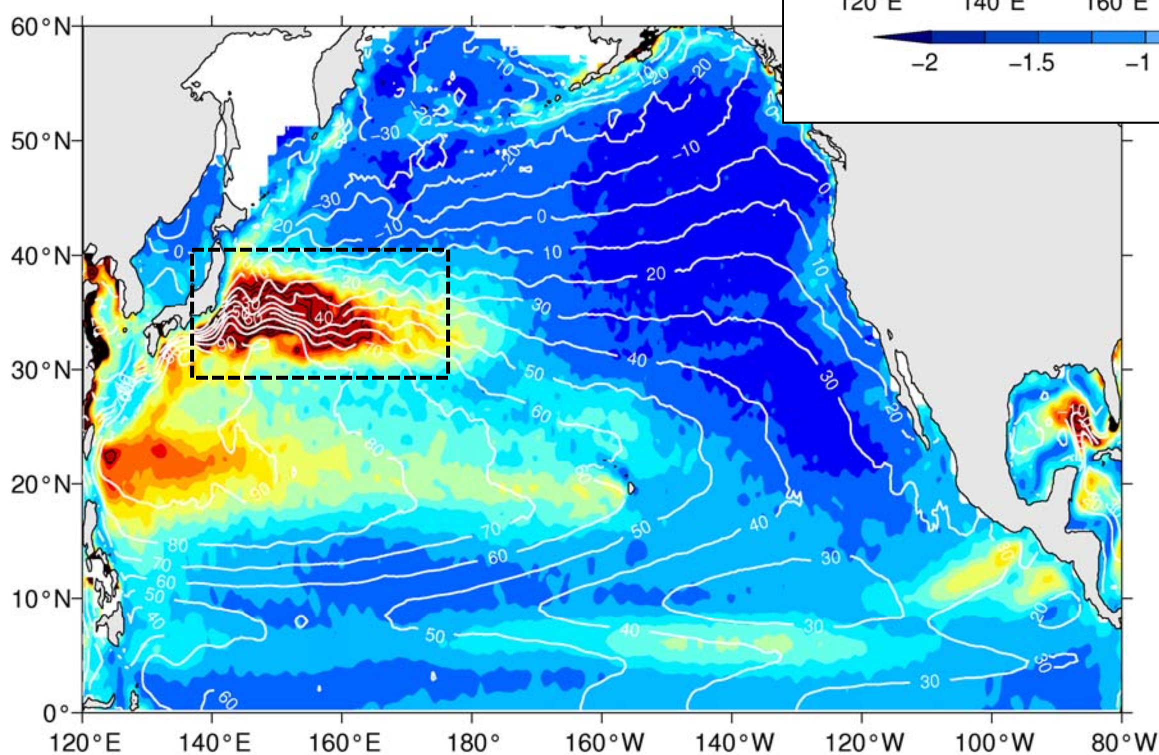

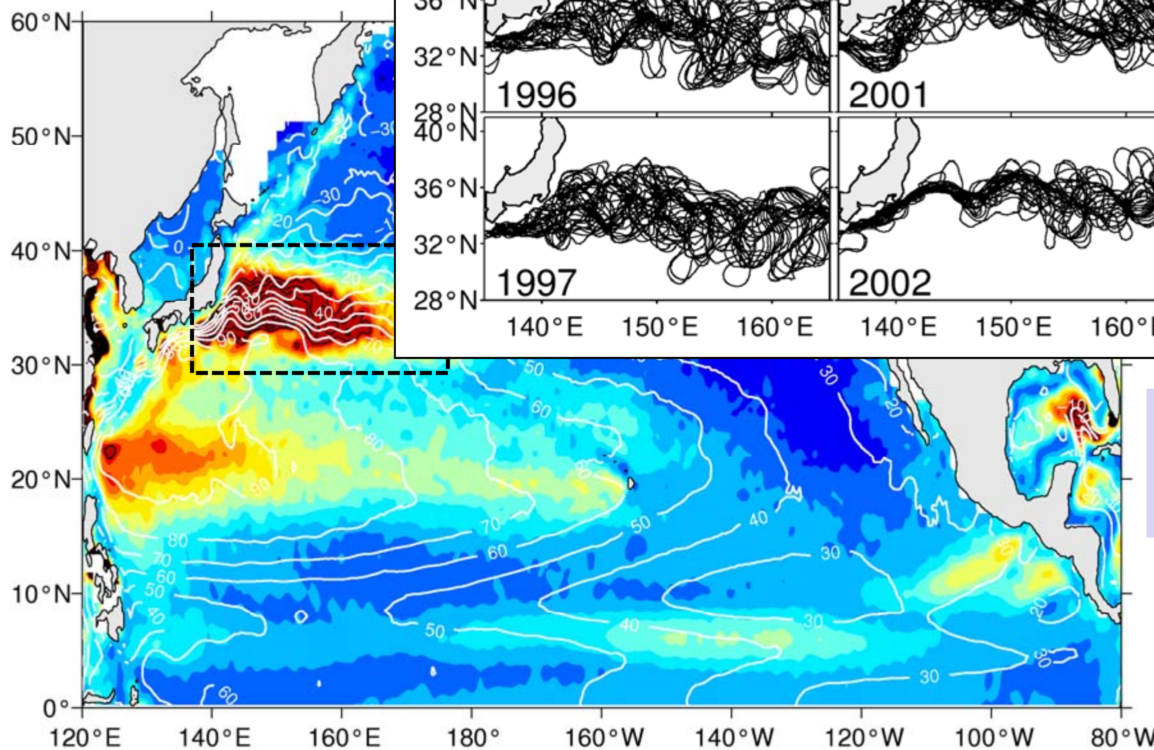

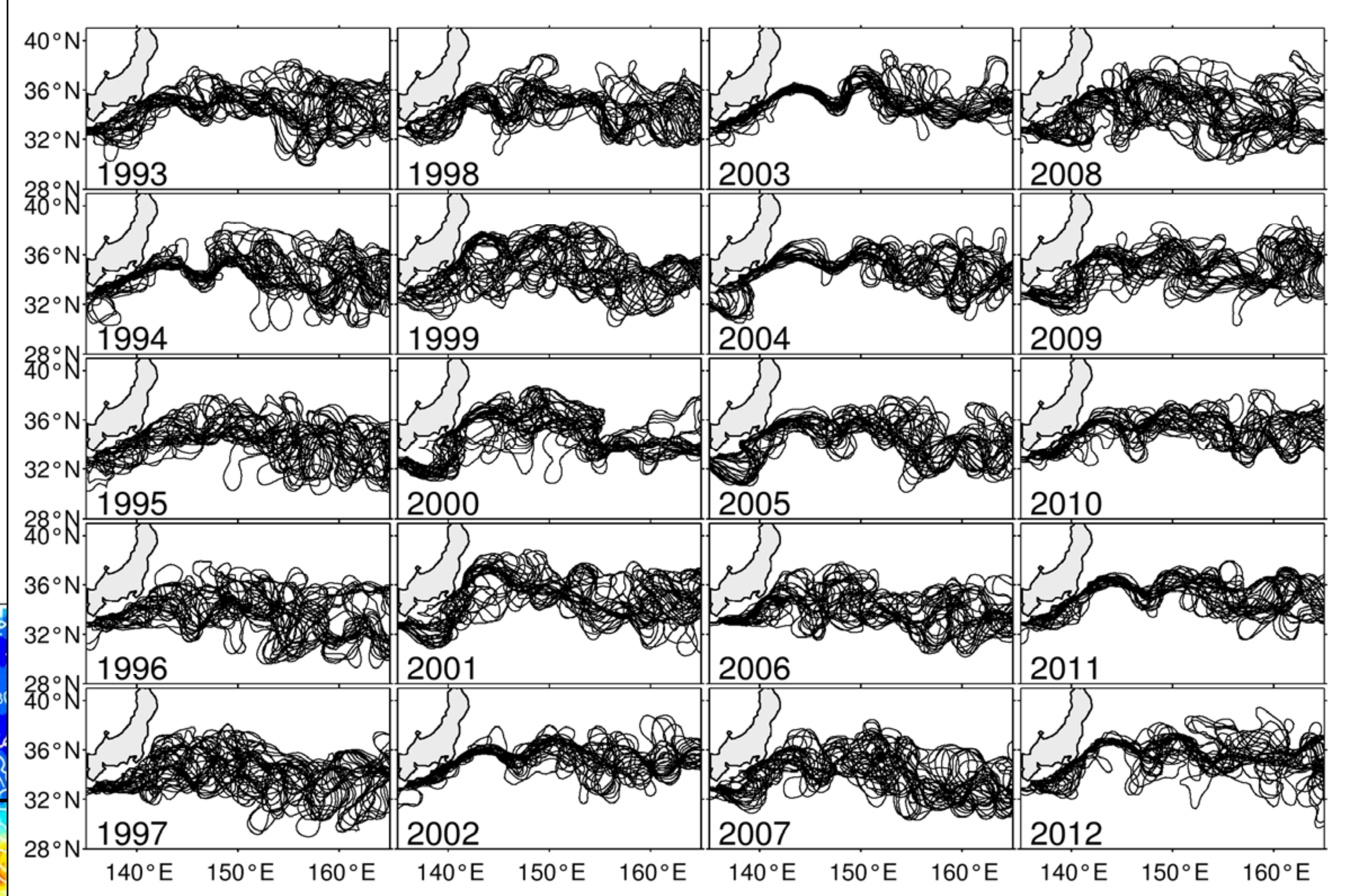

Semi-monthly KE path inferred from AVISO SSH field

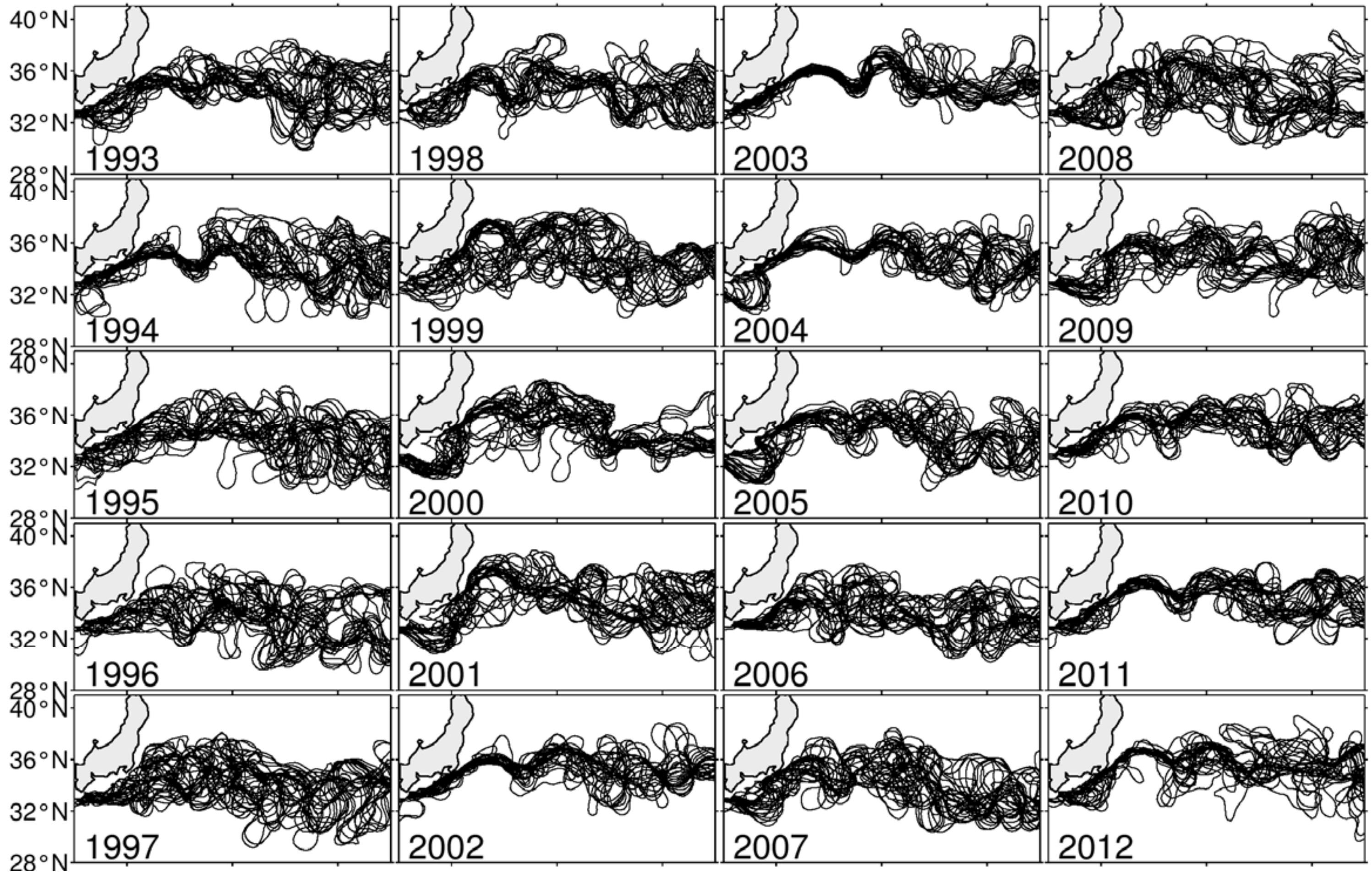

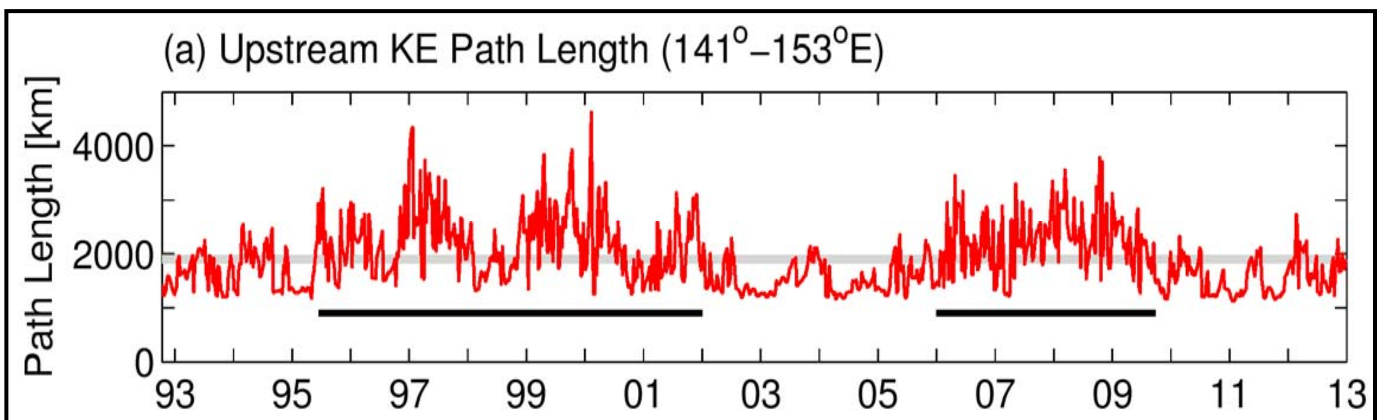

Stable yrs: 1993-94, 2002-04, 2010-2013

Unstable yrs: 1996-2001, 2006-08

Yearly SSH maps: path stability represents one aspect of the bimodal KE system

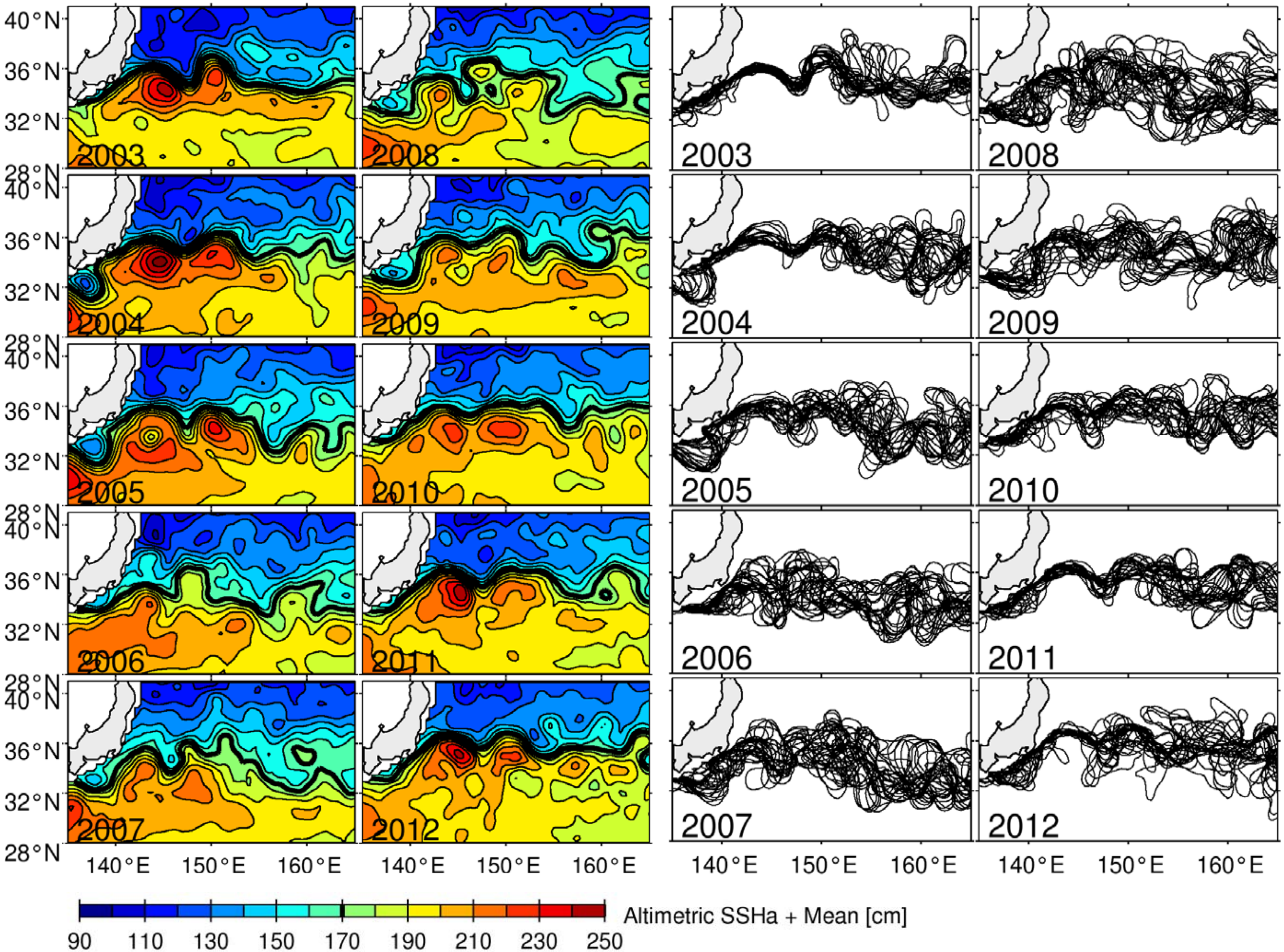

Decadal KE variability lags the PDO index by ~ 4 yrs (r = 0.50)

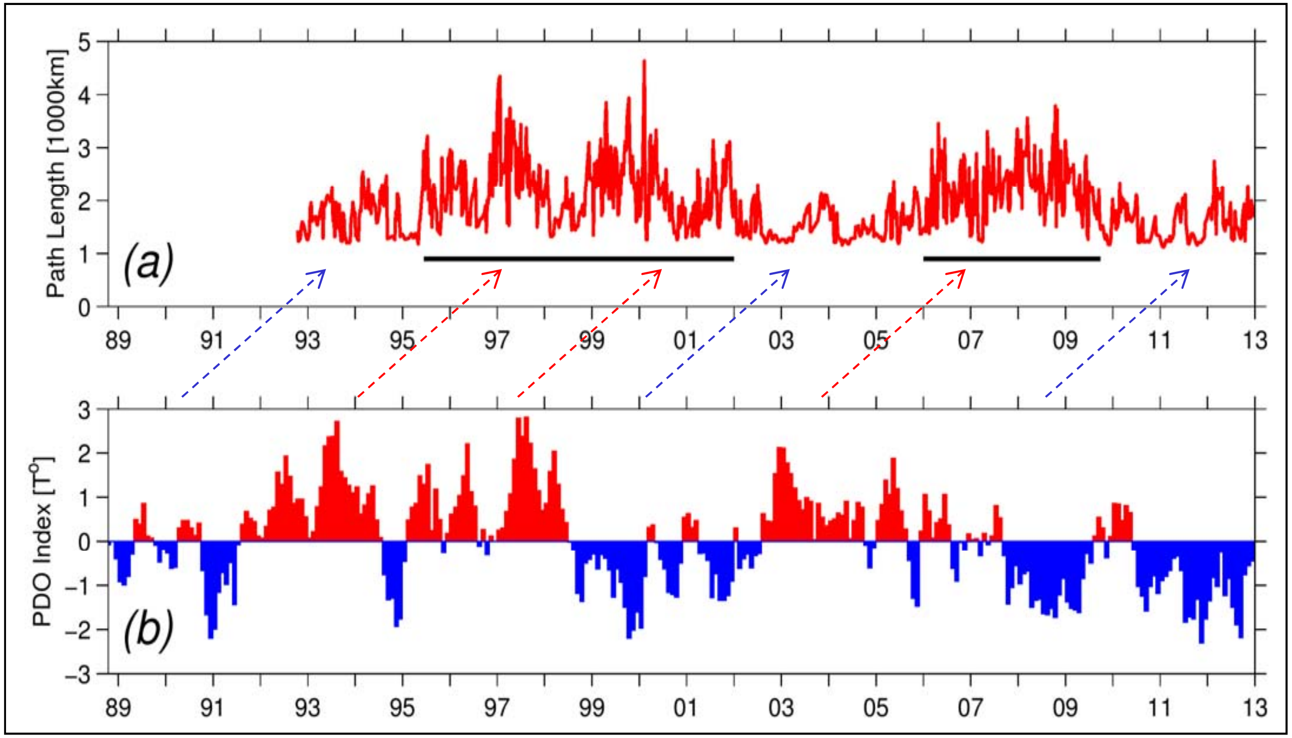

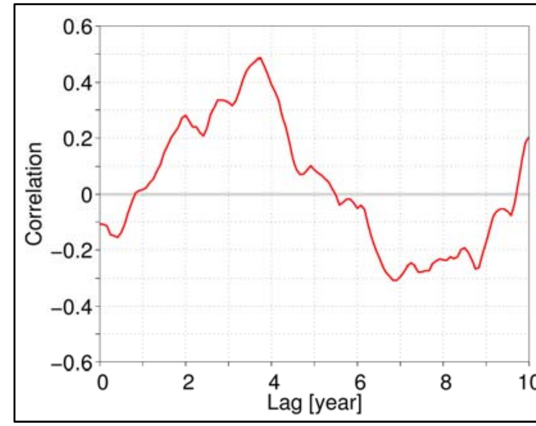

- Center of PDO forcing is in eastern half of North Pacific basin
- SSH adjustment in midlatitude is via slow baroclinic Rossby waves → ~ 4-year lag
- \+ PDO generates negative local SSHAs through Ekman divergence, and vice versa

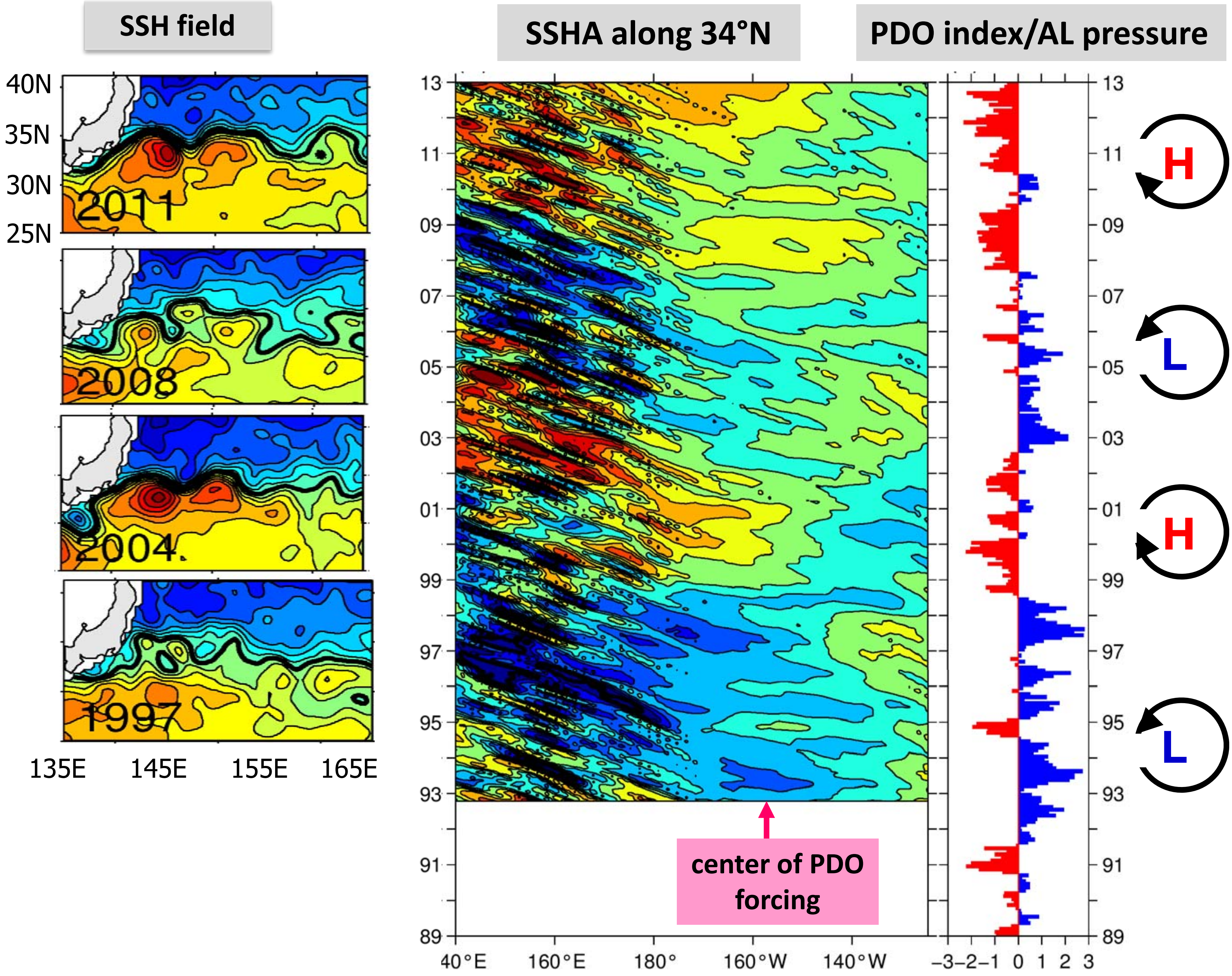
SSH field
SSHA along 34°N
PDO index/AL pressure
40N
35N
30N
25N
2011
2008
2004
1997
135E
145E
155E
165E
13
11
09
07
05
03
01
99
97
95
93
91
89
40°E
160°E
180°
160°W
140°W
−3 −2 −1 0 1 2 3
H
L
H
L
center of PDO forcing

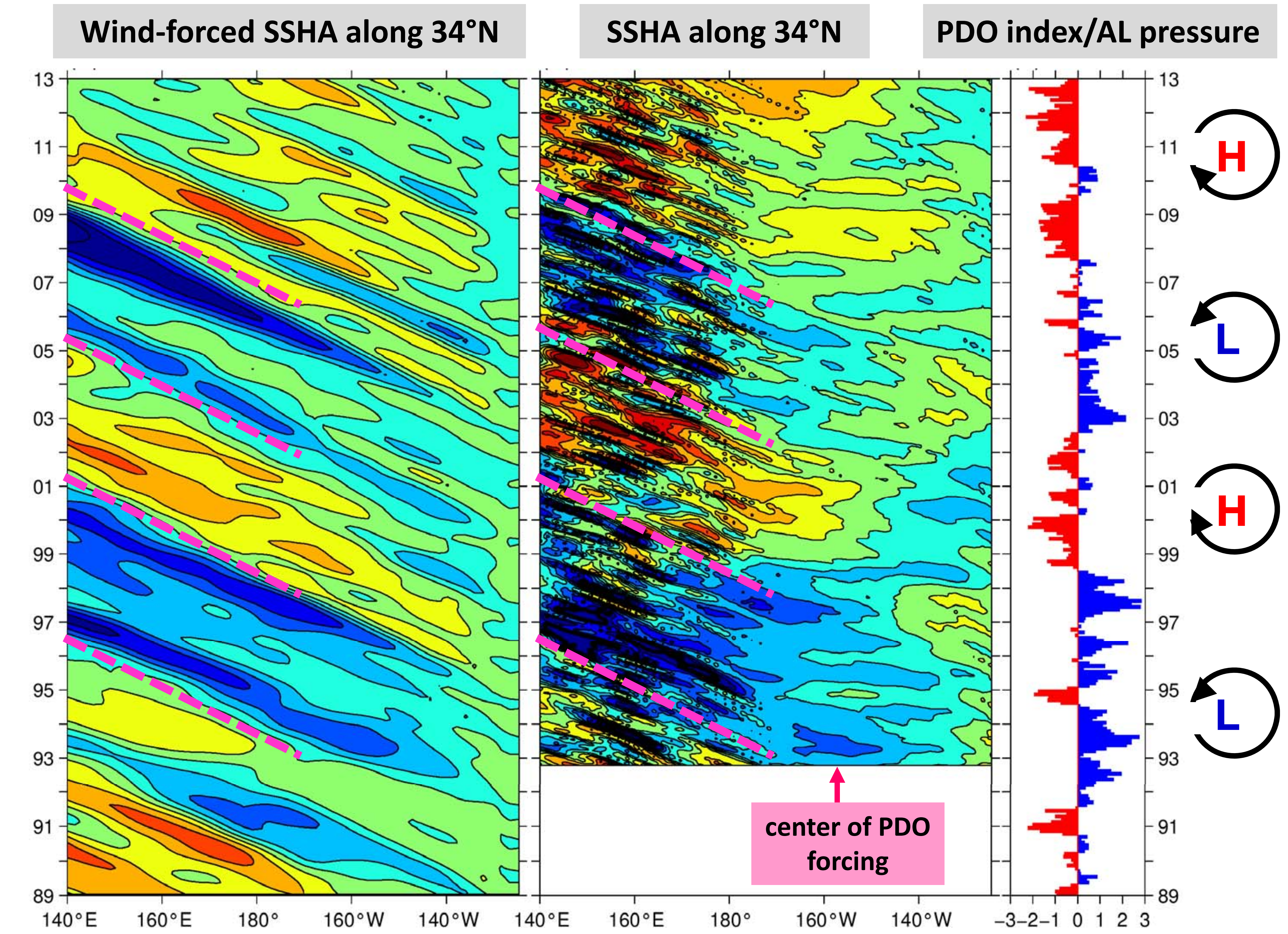

Wind-forced SSHA along 34°N
SSHA along 34°N
PDO index/AL pressure
13
11
09
07
05
03
01
99
97
95
93
91
89
140°E
160°E
180°
160°W
140°W
−3 −2 −1 0 1 2 3
H
L
H
L
center of PDO forcing

Summary

- While all affected by PDO wind forcing, different current systems respond differently according to their underlying dynamics.
- For the bifurcating NEC in low-latitudes, wind response is fast and persistent Ekman flux convergence off the Philippines leads to steady southward shift of tropical-subtropical gyre boundary.
- Along the STCC band, overlying PDO-related wind stress curl forcing modifies upper ocean baroclinic shear, inducing decadal changes in level of mesoscale eddies.
- In mid-latitudes, slow baroclinic Rossby wave adjustment causes a delayed response (of ~ 4 years) in dynamical state changes of the KE system.

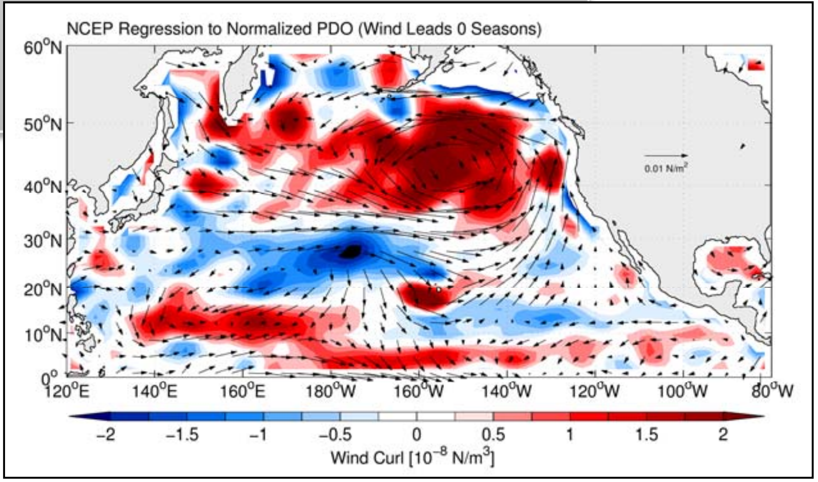

The reason behind enhanced predictive skill with the 4~6 yr lead:
delayed negative feedback mechanism

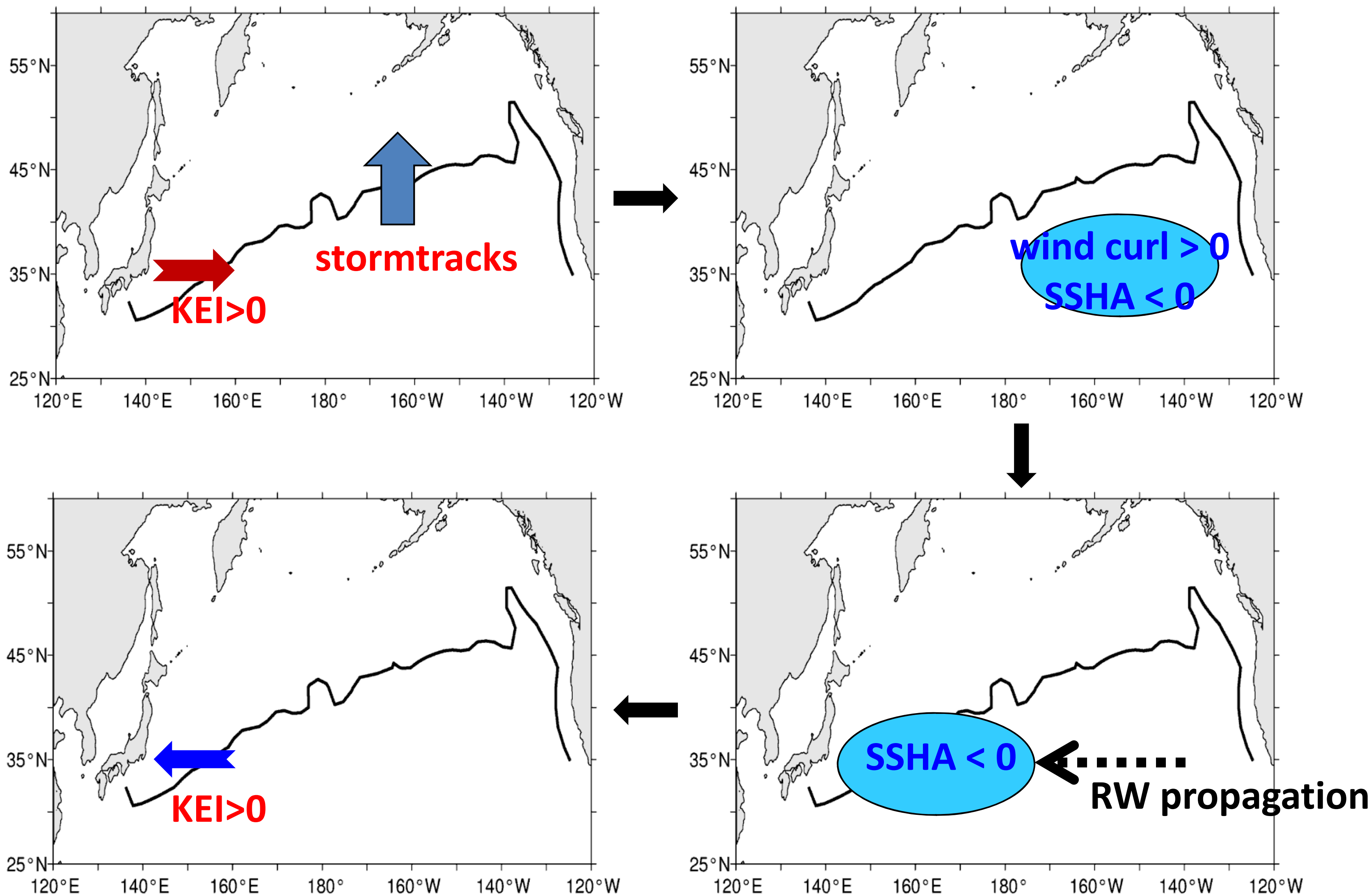

half of the oscillation cycle: ~5 yrs in the N Pacific basin

Quantifying the surface wind and heat flux forcing on $\partial U_g/\partial z$ changes

- **From the thermal wind relation:**

$$\langle \frac{\partial U_g}{\partial z} \rangle = -\frac{\alpha g}{f} \frac{\partial \langle T \rangle}{\partial y}$$

where $\langle\,\rangle$ denote the depth average in the 150m upper ocean.

- **Temperature budget equation in the 150m upper ocean:**

$$\frac{\partial \langle T \rangle}{\partial t} = -\langle \mathbf{u}_{Ek} \rangle \cdot \nabla \langle T \rangle + \frac{Q_{net}}{\rho_0 c_p H_0} + \text{other terms}$$

where $\mathrm{k} \times \langle \mathbf{u}_{Ek} \rangle = \boldsymbol{\tau}/\rho_0 f H_0$ and "other terms" include geostrophic advection, entrainment, and eddy diffusion.

- **Combine:**

$$\frac{\partial}{\partial t}\left(\langle \frac{\partial U_g}{\partial z} \rangle \right) = \frac{\alpha g}{f} \frac{\partial}{\partial y} \left(\langle \mathbf{u}_{Ek} \rangle \cdot \nabla \langle T \rangle \right) - \frac{\alpha g}{f \rho_0 c_p H_0} \frac{\partial Q_{net}}{\partial y} + \text{other terms}$$

Ekman flux convergence

y-dependent Q_{net} forcing

$\partial U_g/\partial z$ vs. time-integrated forcing in 18-28°N, 125°E-150°W

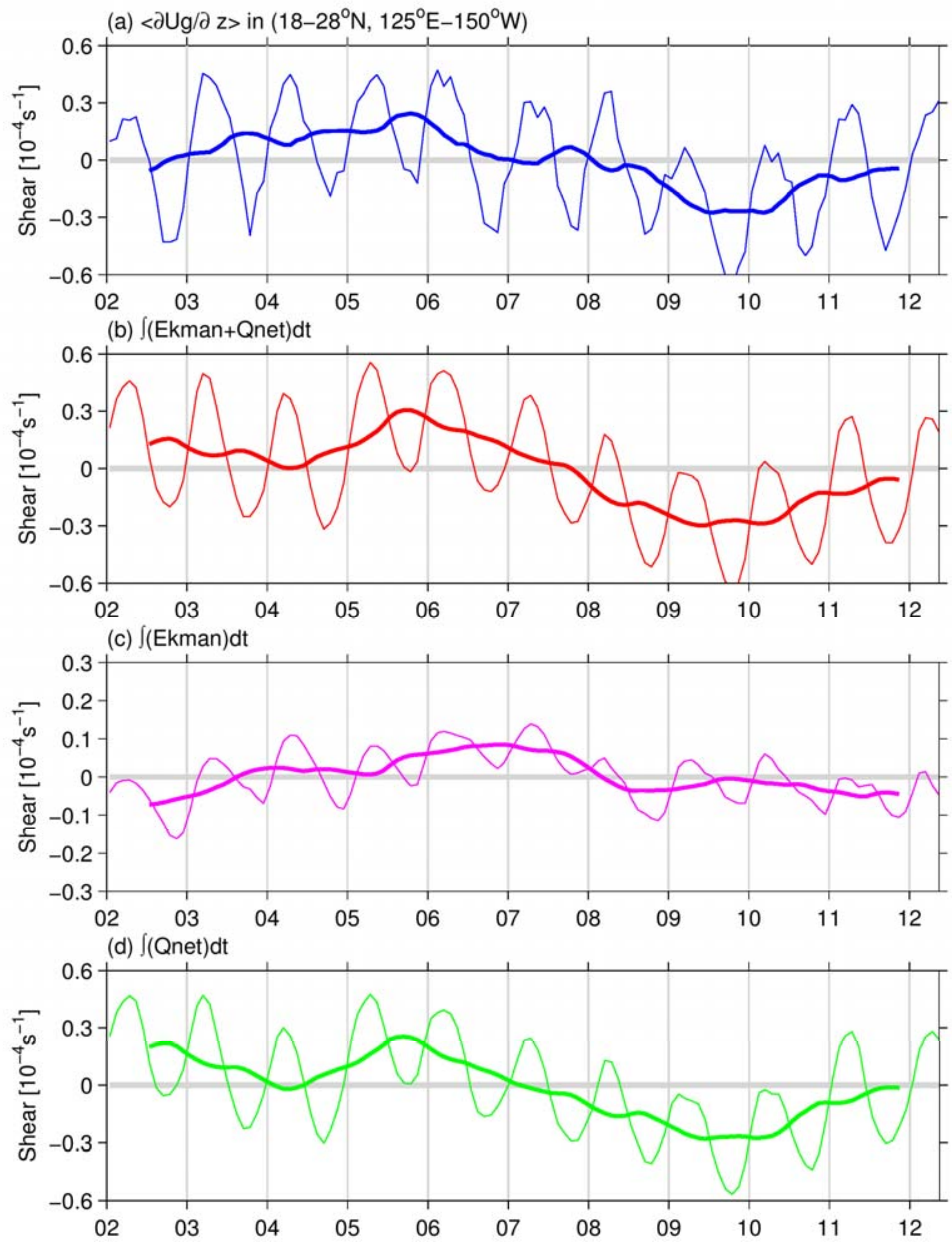

$\langle \partial U_g/\partial z \rangle$

Ekman flux + Q_{net} forcing

Ekman flux convergence

y-dependent Q_{net} forcing

Various dynamic properties representing the decadal KE variability

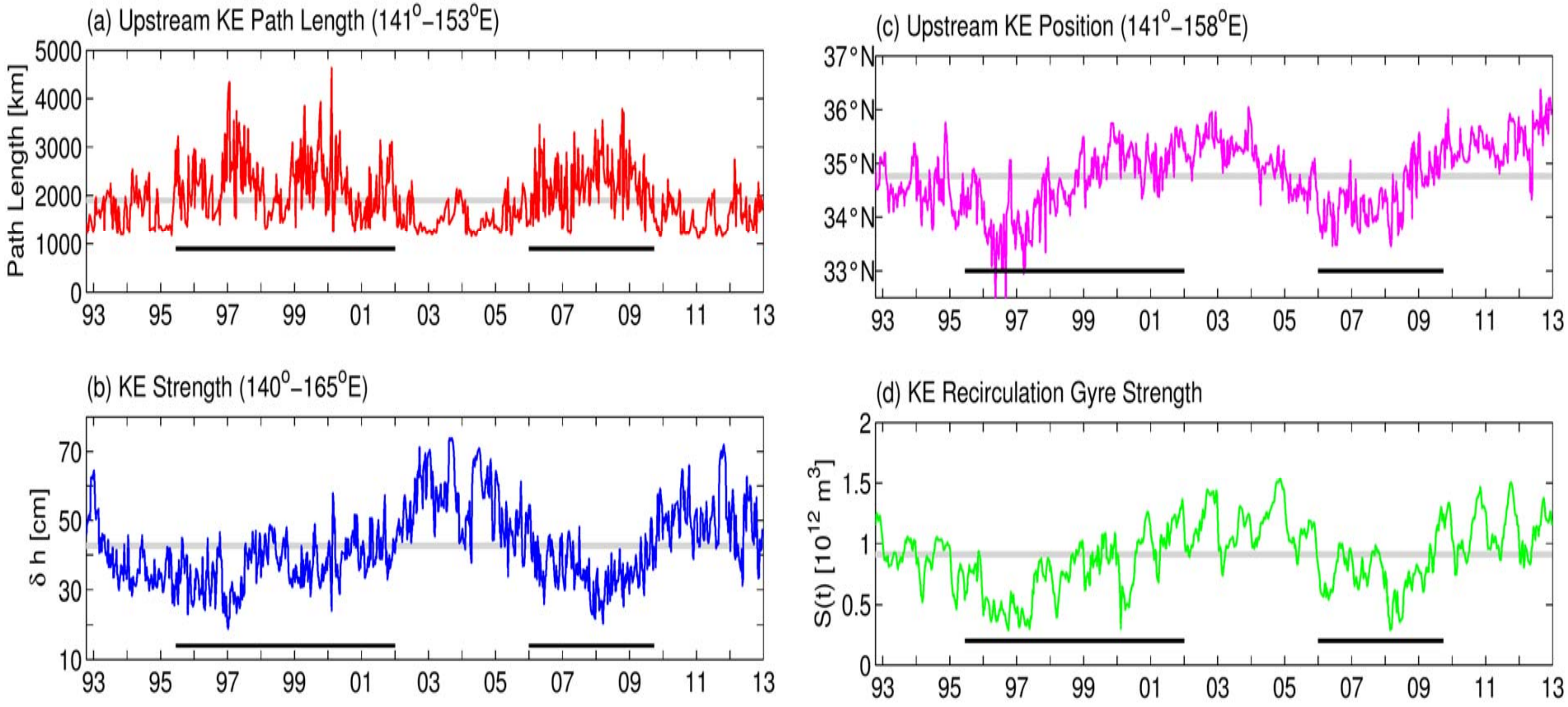

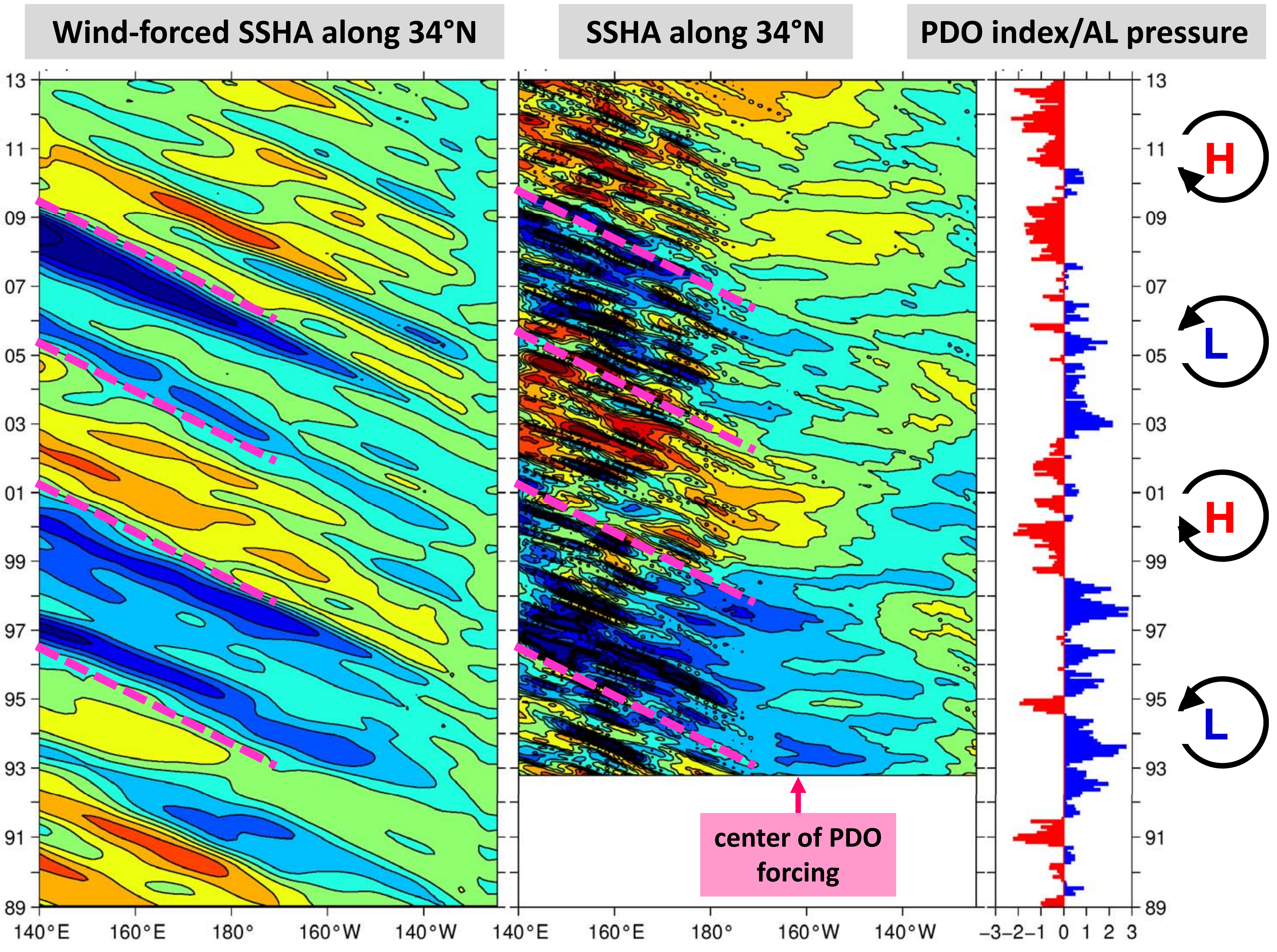

Wind-forced SSHA along 34°N
SSHA along 34°N
PDO index/AL pressure
13
11
09
07
05
03
01
99
97
95
93
91
89
140°E
160°E
180°
160°W
140°W
-3 -2 -1 0 1 2 3
H
L
H
L
center of PDO forcing